AGU PUBLICATIONS

Global Biogeochemical Cycles

RESEARCH ARTICLE
10.1002/2014GB005013

Key Points:
- Low nitrate $\delta^{15}N$ and $\delta^{15}N/\delta^{18}O$ reveal Antarctic winter mixed layer nitrification
- Data explain the anomalous nitrate $\delta^{15}N/[NO_3^-]$ relationship in the summer T_{min}
- Low $\delta^{15}N$ winter mixed layer nitrate implies intense late summer ammonium cycling

Supporting Information:
- Readme
- Texts S1 and S2
- Figure S1
- Figure S2
- Figure S3
- Figure S4

Correspondence to:
S. M. Smart,
sandimsmart@gmail.com

Citation:
Smart, S. M., S. E. Fawcett, S. J. Thomalla, M. A. Weigand, C. J. C. Reason, and D. M. Sigman (2015), Isotopic evidence for nitrification in the Antarctic winter mixed layer, *Global Biogeochem. Cycles*, *29*, 427–445, doi:10.1002/2014GB005013.

Received 13 OCT 2014
Accepted 16 MAR 2015
Accepted article online 21 MAR 2015
Published online 22 APR 2015

Isotopic evidence for nitrification in the Antarctic winter mixed layer

Sandi M. Smart[1], Sarah E. Fawcett[2], Sandy J. Thomalla[1,3], Mira A. Weigand[2], Chris J. C. Reason[1], and Daniel M. Sigman[2]

[1]Department of Oceanography, University of Cape Town, Rondebosch, South Africa, [2]Department of Geosciences, Princeton University, Princeton, New Jersey, USA, [3]Ocean Systems and Climate Group, Council for Scientific and Industrial Research, Stellenbosch, South Africa

Abstract We report wintertime nitrogen and oxygen isotope ratios ($\delta^{15}N$ and $\delta^{18}O$) of seawater nitrate in the Southern Ocean south of Africa. Depth profile and underway surface samples collected in July 2012 extend from the subtropics to just beyond the Antarctic winter sea ice edge. We focus here on the Antarctic region (south of 50.3°S), where application of the Rayleigh model to depth profile $\delta^{15}N$ data yields estimates for the isotope effect (the degree of isotope discrimination) of nitrate assimilation (1.6–3.3‰) that are significantly lower than commonly observed in the summertime Antarctic (5–8‰). The $\delta^{18}O$ data from the same depth profiles and lateral $\delta^{15}N$ variations within the mixed layer, however, imply O and N isotope effects that are more similar to those suggested by summertime data. These findings point to active nitrification (i.e., regeneration of organic matter to nitrate) within the Antarctic winter mixed layer. Nitrite removal from samples reveals a low $\delta^{15}N$ for nitrite in the winter mixed layer (−40‰ to −20‰), consistent with nitrification, but does not remove the observation of an anomalously low $\delta^{15}N$ for nitrate. The winter data, and the nitrification they reveal, explain the previous observation of an anomalously low $\delta^{15}N$ for nitrate in the temperature minimum layer (remnant winter mixed layer) of summertime depth profiles. At the same time, the wintertime data require a low $\delta^{15}N$ for the combined organic N and ammonium in the autumn mixed layer that is available for wintertime nitrification, pointing to intense N recycling as a pervasive condition of the Antarctic in late summer.

1. Introduction

The balance between summertime major nutrient (nitrate and phosphate) consumption and wintertime nutrient recharge is central to the role of the Antarctic in setting atmospheric CO_2 levels [*Sarmiento and Toggweiler*, 1984] and global nutrient distributions [*Sarmiento et al*., 2004]. Biogeochemical studies of the summertime Antarctic are frequently compromised by limited knowledge of the preceding wintertime conditions, as it is the winter that sets the initial conditions for spring and summer growth. Characterizing this wintertime state is therefore an important stepping stone toward understanding the role of the Southern Ocean in the carbon cycle, global climate, and ocean fertility.

The Antarctic Zone (AZ) lies south of the Polar Front (PF) and is often subdivided by the Southern Antarctic Circumpolar Current Front (SACCF) into a northern and a southern domain: the Open Antarctic Zone (OAZ, which is "ice-free" year round) and the Polar Antarctic Zone (PAZ, which typically experiences seasonal ice cover) [*Whitworth*, 1980; *Orsi et al*., 1995]. The bulk of the Southern Ocean interior is occupied by Circumpolar Deep Water (CDW), which can be subdivided into an upper (UCDW) and a lower (LCDW) layer [*Whitworth and Nowlin*, 1987]. UCDW is distinguished from LCDW by its higher nitrate concentration ($[NO_3^-]$) and lower dissolved oxygen content, stemming from lateral communication with the Indian and Pacific basins [*Callahan*, 1972; *Park et al*., 1993; *Orsi et al*., 1995]. LCDW, as a result of North Atlantic Deep Water incorporation, has higher salinities, lower $[NO_3^-]$, and higher oxygen content than UCDW [*Whitworth and Nowlin*, 1987].

Nitrate is supplied to the AZ summer mixed layer by two main mechanisms: (1) Ekman divergence, which drives upwelling, and (2) wintertime cooling (plus sea ice formation in the PAZ), which increases the density of surface waters, promoting convective overturning and a deepening of the mixed layer. Mixed layer deepening mixes what was summertime surface water down into the subsurface to a depth of ~150 m by late winter. The water below the summertime mixed layer exchanges with underlying CDW throughout the year, such that wintertime deep mixing effectively imports CDW into the mixed layer. In the summer,

warming and melting cause the surface wind-mixed layer to become shallower, leaving the remnant base of the winter mixed layer behind as what is known as the temperature minimum (T_{min}) layer [*Gordon et al*., 1977]. The T_{min} is thought of as a summertime record of wintertime conditions, an assumption that has been tested at only a few AZ sites [*Altabet and François*, 2001; *DiFiore et al*., 2010]. In the PAZ, where UCDW is absent from the subsurface or less distinct from LCDW, the winter mixed layer seems to be fed predominantly by LCDW [*Whitworth and Nowlin*, 1987; *DiFiore et al*., 2010]. In the OAZ, UCDW is found directly below the T_{min}, suggesting it to be the dominant nitrate source to surface waters in this region. However, lateral exchange with the PAZ may lead to indirect supply of LCDW nitrate to the OAZ [*DiFiore et al*., 2010] (and, reciprocally, some contribution of UCDW to the PAZ). One physical sign of OAZ/PAZ lateral exchange is that the remnant winter mixed layer observed in the summertime PAZ often represents a depth maximum in temperature, known as the "T_{max}" layer [*Bindoff et al*., 2000].

Natural variations in the nitrogen isotope ratios ($^{15}N/^{14}N$) of nitrate can be used to trace various processes in the marine nitrogen cycle, including the assimilation of nitrate by phytoplankton [*Altabet and François*, 1994a; *Sigman et al*., 1999; *Trull et al*., 2008; *Sigman et al*., 2009a]. By convention, N isotopic composition is expressed in delta notation ($\delta^{15}N$; in units of per mil, ‰) relative to atmospheric N_2, where $\delta^{15}N = \{[(^{15}N/^{14}N)_{sample}/(^{15}N/^{14}N)_{atmN2}] - 1\} \times 1000$. In the AZ summertime upper ocean, the dominant signal in the $\delta^{15}N$ of nitrate is the kinetic isotope fractionation associated with nitrate assimilation. Given the finite nitrate pool in the relatively well-isolated AZ summer mixed layer, preferential incorporation of ^{14}N-bearing nitrate causes the remaining nitrate pool to become progressively enriched in ^{15}N [*Sigman et al*., 1999]. The degree of N isotopic fractionation is quantified as the "isotope effect" of nitrate assimilation ($^{15}\varepsilon_{assim}$; in units of per mil, ‰), defined here as $^{15}\varepsilon_{assim} = (^{14}k/^{15}k - 1) \times 1000$, where ^{14}k and ^{15}k are the reaction rate coefficients for assimilation of ^{14}N- and ^{15}N-bearing nitrate, respectively.

If nitrate consumption proceeds with a constant isotope effect and if there are no significant mechanisms of nitrate resupply during the summer period of stratification and phytoplankton growth, the isotope systematics can be described using the Rayleigh model [*Mariotti et al*., 1981]. Under these conditions, the $\delta^{15}N$ of the remaining nitrate pool ($\delta^{15}N_{reactant}$) is described by the (approximate) equation:

$$\delta^{15}N_{reactant} = \delta^{15}N_{initial} - {}^{15}\varepsilon_{assim} \cdot \ln(f) \quad (1)$$

where $\delta^{15}N_{initial}$ refers to the starting $\delta^{15}N$ of the nitrate being consumed, $^{15}\varepsilon_{assim}$ is the N isotope effect of nitrate assimilation, and *f* is the fraction of nitrate remaining (calculated as $[NO_3^-]/[NO_3^-]_{initial}$). Thus, if nitrate drawdown in the AZ follows closed-system dynamics, then upper ocean nitrate samples should fall along a straight line in "Rayleigh space" (with nitrate $\delta^{15}N$ plotted against the natural log of $[NO_3^-]$), where the slope of the line approximates $^{15}\varepsilon_{assim}$ [*Mariotti et al*., 1981; *Sigman et al*., 1999].

While it is natural to be suspicious of the applicability of the Rayleigh model's criterion of no nitrate resupply during consumption, this is not an overriding concern in the modern AZ. This is because at the low degrees of nitrate consumption that apply in the AZ (30% or less), resupply does not cause nitrate $\delta^{15}N$ to diverge significantly from the Rayleigh relationship with $[NO_3^-]$ [*Sigman et al*., 1999].

Even so, summertime nitrate isotope data from the Indian and Pacific sectors of the AZ indicate the existence of processes that complicate their interpretation within the framework of the Rayleigh model. In the coastal PAZ, nitrate $\delta^{15}N$ shows no obvious deviations from the Rayleigh-predicted relationship with $[NO_3^-]$, extending along a Rayleigh-consistent line in $\delta^{15}N$ versus $\ln([NO_3^-])$ space from underlying LCDW into the summertime mixed layer [*DiFiore et al*., 2009]. Best-fit slopes connecting the PAZ summer mixed layer with LCDW at depth indicate an $^{15}\varepsilon_{assim}$ of ~5‰ (slope of the solid grey line in Figure 1). OAZ profiles, in contrast, exhibit a distinct deviation from the expected Rayleigh trend. In $\delta^{15}N$ versus $\ln([NO_3^-])$ space, data from the T_{min} layer fall well below the linear trend that would connect the OAZ summer mixed layer with UCDW at depth [*Sigman et al*., 1999] (compare black symbols with dashed line in Figure 1). We refer to this T_{min} feature as a "kink" in the OAZ trend in Rayleigh space.

The cause of the kink is unknown. *DiFiore et al*. [2010] proposed that the T_{min} anomaly of the OAZ is best explained by lateral exchange with the T_{max} layer of the PAZ. The nitrate properties of the T_{max} layer are largely consistent with the expectations of nitrate assimilation from a LCDW source (~4.8‰ at 33 μM) [*Sigman et al*., 2000]. The T_{min} layer might receive its nitrate from either the adjacent PAZ T_{max} layer or

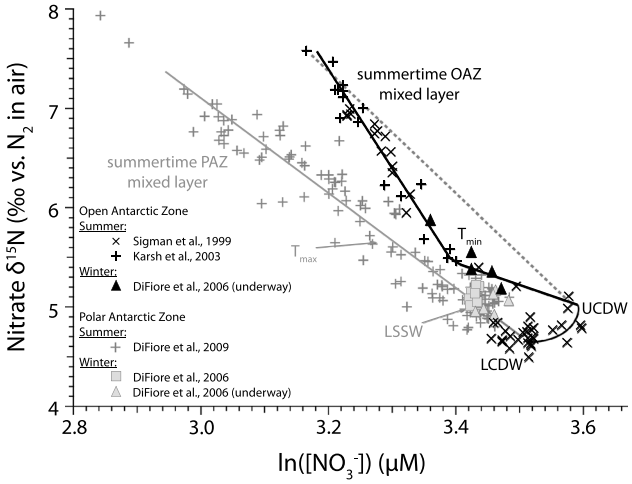

Figure 1. Compilation of winter and summer AZ data from south of Australia plotted in nitrate $\delta^{15}N$ versus ln($[NO_3^-]$) space (OAZ in black and PAZ in grey). The solid symbols represent winter data, while the + signs and x signs denote summer data. The solid grey and black lines indicate the depth progression through the data in the PAZ and OAZ, respectively, along which key water masses are labeled (see text for acronym definitions). The dashed grey line indicates the expected trajectory for OAZ summer profiles assuming that nitrate available for drawdown in the early summer has the $[NO_3^-]/\delta^{15}N$ relationship of pure UCDW, an assumption that appears to be falsified by the chemistry of the OAZ T_{min}. Original data sources are indicated in the bottom left (source: *DiFiore et al.* [2010]).

underlying UCDW, the latter having a higher $\delta^{15}N$ for its $[NO_3^-]$ (~5.3‰ at 35 μM in the OAZ) due to its communication with mid-depth low-latitude Indo-Pacific waters [*Sigman et al.*, 2000; *Sigman et al.*, 2009b; *Rafter et al.*, 2013]. The low $\delta^{15}N$ of OAZ T_{min} samples from south of Australia has been interpreted as indicating that lateral exchange with the PAZ accounts for the greater part (~60%) of the OAZ T_{min} nitrate in this region [*DiFiore et al.*, 2010].

These uncertainties with regard to the ultimate nitrate source to the OAZ upper ocean and the processes that generate the observed summertime T_{min} properties affect the interpretation of the N isotope data from the summertime surface OAZ. Assuming UCDW as the source yields low estimates for $^{15}\varepsilon_{assim}$, in the range of 4–6‰ [*Sigman et al.*, 1999] (slope of the dashed grey line in Figure 1), while using the summertime T_{min} as the source (with its chemistry explained by lateral exchange in the upper ocean or some other process) leads to higher estimates of 7–9‰ [*DiFiore et al.*, 2010] (slope of the solid black line between "T_{min}" and "summertime OAZ mixed layer" in Figure 1). This complication does not arise in the coastal PAZ, where all potential nitrate sources to the summertime surface—LCDW, Low-Salinity Shelf Water (LSSW, which also derives from LCDW), and for the most part, the T_{max} layer—fall along the same Rayleigh nutrient utilization trend (solid grey line in Figure 1), such that the choice of initial values has minimal impact on the $^{15}\varepsilon_{assim}$ estimates [*DiFiore et al.*, 2009].

Based on a comparison of data from three cruises south of Australia, *DiFiore et al.* [2010] find only modest changes in nitrate $\delta^{15}N$ and concentration as the OAZ winter mixed layer evolves into the summertime T_{min} layer. This suggests that the T_{min} is a good reflection of the nitrate available for consumption at the beginning of the spring/summer growth period in the OAZ, consistent with other data from south of New Zealand [*Altabet and François*, 2001], and consequently provides support for a higher $^{15}\varepsilon_{assim}$ in the OAZ (≥7‰). However, the evidence is currently too thin for us to be confident that the T_{min} reflects the springtime nitrate source across the entire OAZ, with consequences for all aspects of the interpretation of summertime nitrate concentration and isotope data. Furthermore, the kink itself is a major feature that has parallels in other polar regions, including the Bering Sea [*Brunelle*, 2009]. Thus, its origin may reveal as yet unidentified biogeochemical and/or circulation processes in the polar ocean in general.

Deviations from a single nitrate consumption/nitrate $\delta^{15}N$ relationship have been investigated most intensively in the Subantarctic Zone (SAZ, between the Subtropical Front (STF) and the Subantarctic Front (SAF)), where they reflect the effect of mixing between nitrate-rich and nitrate-poor waters [*Sigman et al.*, 1999; *DiFiore et al.*, 2006]. Furthermore, constraints provided by the O isotopes of nitrate ($\delta^{18}O$, in units of per mil, ‰, versus Vienna Standard Mean Ocean Water (VSMOW); defined as $\delta^{18}O = \{[(^{18}O/^{16}O)_{sample}/(^{18}O/^{16}O)_{VSMOW}] - 1\} \times 1000$) have allowed for additional non-assimilation processes to be identified. A deviation from the nitrate $\delta^{18}O$-to-$\delta^{15}N$ relationship expected for nitrate assimilation alone (a 1:1 relationship since $^{18}\varepsilon_{assim}/^{15}\varepsilon_{assim} \approx 1$ [*Granger et al.*, 2004]) has been shown to result from an internal cycle within the SAZ that includes summertime partial nitrate assimilation in the surface, remineralization of sinking N in the thermocline, and resupply of thermocline nitrate to the surface during winter mixing [*Rafter et al.*, 2013].

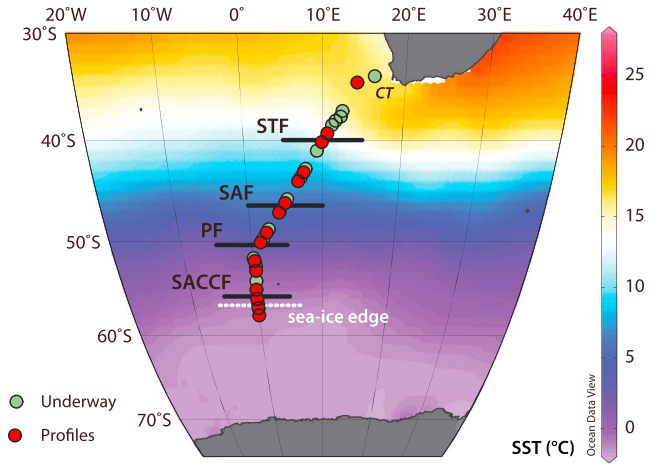

Figure 2. Map of the July 2012 cruise track along the Good Hope Line from Cape Town (CT) to the sea ice edge (white dashed line). Stations sampled during the cruise are indicated by the circles (underway stations in green and hydrocast stations in red), plotted against July sea surface temperature climatology (in °C) from World Ocean Atlas 2009 (http://www.nodc.noaa.gov/OC5/WOA09/pr_woa09.html). The major fronts at the time of sampling are indicated (STF: Subtropical Front, SAF: Subantarctic Front, PF: Polar Front, and SACCF: Southern Antarctic Circumpolar Current Front).

Here we report the first nitrate $\delta^{15}N$ and $\delta^{18}O$ data from the Southern Ocean south of Africa, providing the most comprehensive view to date of nitrate isotopes in the wintertime Antarctic. After presenting the full data set, which spans a latitude range of 33.9°S to 57.8°S, we narrow our focus to the AZ (south of 50.3°S). The observations of the AZ winter mixed layer are found to provide an explanation for the T_{min} kink of the summertime Antarctic. Based on evidence from the $\delta^{18}O$ and $\delta^{15}N$ of nitrate, we suggest that this kink is the combined result of late summer N recycling and subsequent wintertime nitrification within the mixed layer of the AZ. Finally, we consider the implications of our findings for Antarctic nitrate dynamics.

2. Methods

2.1. Cruise Track and Hydrographic Setting

The data presented here derive from the wintertime voyage of the R/V *S.A. Agulhas II* (VOY03) from Cape Town (33.9°S, 18.4°E), South Africa, along the Good Hope monitoring line [*Ansorge et al*., 2005] into the wintertime sea ice (encountered at 56.7°S) in July 2012 (Figure 2). Twenty-two hydrocasts (to depths of 1000 m or 2000 m) were undertaken on this transect, with the northernmost station in the subtropics at 34.6°S and the southernmost station located in the sea ice at 57.8°S. The major circumpolar fronts were identified from surface and subsurface (200 m) temperature and salinity properties [*Belkin and Gordon*, 1996; *Holliday and Read*, 1998] (positions shown in Figure 2) using data obtained from a Sea-Bird conductivity-temperature-depth (CTD) sensor mounted on the Niskin bottle rosette, as well as from 28 underway-CTD and 88 expendable bathythermograph deployments [*Ansorge*, 2012]. Mixed layer depth was determined from profiles of sigma-theta (σ_θ, calculated from temperature and salinity), with the mixed layer depth at each station defined as the closest depth to the surface at which σ_θ is greater by ≥ 0.03 kg m^{-3} than the value at a reference depth of 32 m (the shallowest depth common to every CTD station) [*de Boyer Montégut et al*., 2004]. Dissolved oxygen profiles (obtained for every CTD cast from a mounted Sea-Bird SBE 43 sensor) were used together with potential density, salinity, and nitrate profiles to identify key water masses.

2.2. Sample Collection

Fifteen of the 22 CTD stations (red dots in Figure 2) were sampled for the $\delta^{15}N$ and $\delta^{18}O$ of dissolved nitrate. From each depth (see Figure 3 for sampling depths), seawater was collected unfiltered in a rinsed 60 mL high-density polyethylene bottle and immediately frozen at −20°C. During the same transect, 60 mL surface seawater samples (green dots in Figure 2) were collected from the ship's underway system (intake at ~7 m) and frozen at −20°C for later analysis; the collected water had passed through a 47 mm diameter in-line filter holder loaded with a 0.4 μm pore size polycarbonate filter. No systematic difference is observed in the isotopic composition of nitrate for filtered and unfiltered seawater samples collected at the same underway sites on a separate leg of the cruise (Figure S1 in the supporting information)—an important observation since underway samples were filtered while profile samples were not.

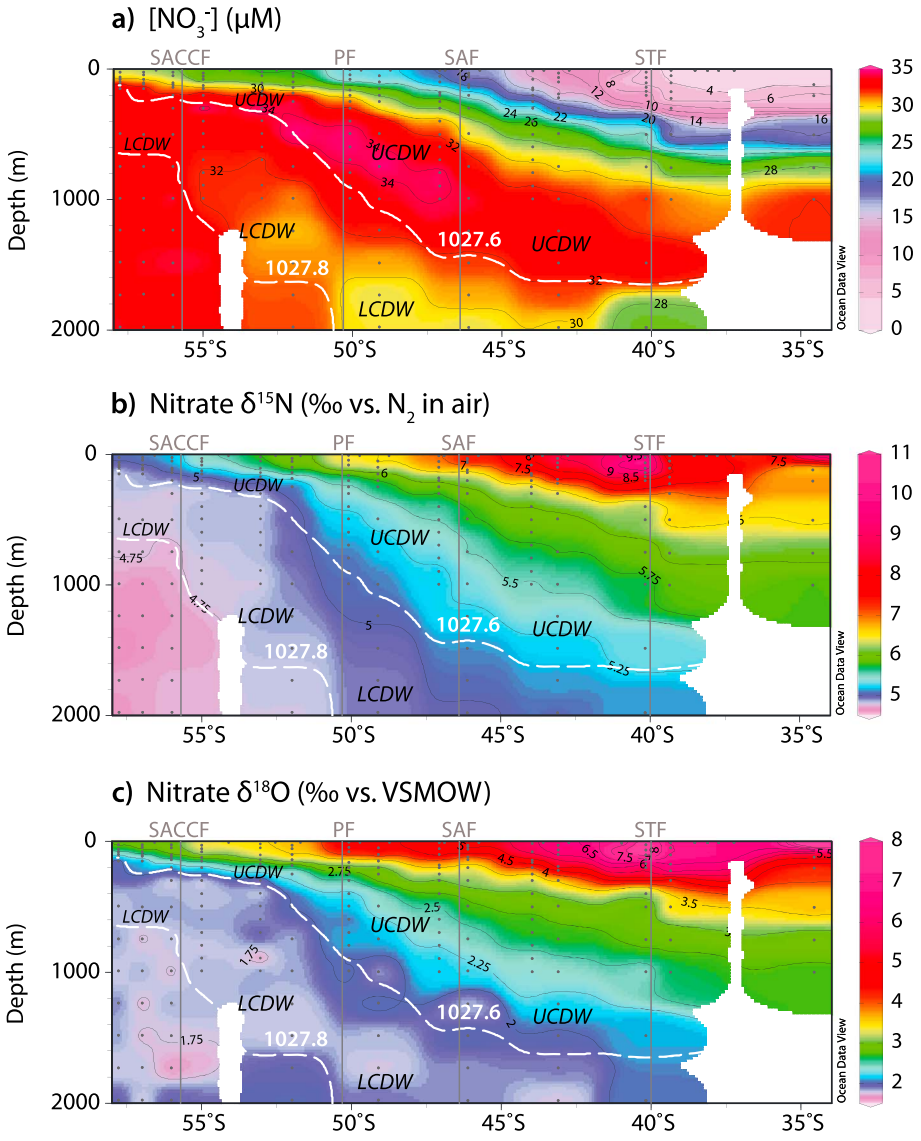

Figure 3. Cross sections of (a) [NO_3^-] (μM), (b) nitrate $\delta^{15}N$ (in ‰ versus N_2 in air), and (c) nitrate $\delta^{18}O$ (in ‰ versus VSMOW) for the wintertime transect between Cape Town (33.9°S) and the Antarctic winter sea ice edge (56.7°S). Sections incorporate both underway surface and profile measurements to a depth of 2000 m, with grey dots denoting sampling depths. The color shading and black contours refer to the primary variable. Isopycnals are denoted by dashed white contours and labels to assist in locating key water masses, namely, LCDW (1027.8 kg m^{-3}) and UCDW (1027.6 kg m^{-3}). Frontal positions are indicated by grey vertical lines and labels above the sections. See text for acronym definitions.

2.3. Isotopic Analysis of Nitrate + Nitrite and Nitrate-Only

The $\delta^{15}N$ and $\delta^{18}O$ of nitrate + nitrite were determined using the "denitrifier method" in conjunction with gas chromatography and isotope ratio mass spectrometry [*Sigman et al.*, 2001; *Casciotti et al.*, 2002]. In this method, dissolved nitrate (NO_3^-) and nitrite (NO_2^-) are converted to nitrous oxide gas (N_2O) via naturally occurring denitrifying bacterial strains that lack an active form of the enzyme N_2O reductase. The international nitrate reference materials International Atomic Energy Agency (IAEA)-N3 and U.S. Geological Survey (USGS)-34, as well as an in-house N_2O standard, were incorporated into every run of samples. After correcting for any isotopic "drift" during the run (determined based on the N_2O standards), the N and O isotope ratios measured by the Thermo MAT 253 mass spectrometer were referenced to atmospheric N_2 and VSMOW, respectively, using IAEA-N3 and USGS-34. The pooled sample standard deviation for $\delta^{15}N$

was 0.05‰ and <0.08‰ for more than 90% of the samples ($n = 3–7$); for $\delta^{18}O$, pooled sample standard deviation was 0.17‰ and <0.25‰ in 90% of cases ($n = 3–5$).

Seawater nitrate + nitrite concentrations ($[NO_3^- + NO_2^-]$) and nitrite concentrations ($[NO_2^-]$) were measured on board by flow injection and standard colorimetric analysis [*Strickland and Parsons*, 1972; *Eriksen*, 1997]. Shipboard concentration measurements from the same stations and depths as our collected seawater samples provided information necessary for nitrate + nitrite isotope analysis. The isotope measurement protocol, in turn, yielded information regarding the amount of N in each sample, which provided an additional means by which the sample concentration (i.e., $[NO_3^- + NO_2^-]$) could be determined. These denitrifier-based $[NO_3^- + NO_2^-]$ data (with a standard error of 0.2 μM on average and <0.4 μM for over 95% of the samples, where $n = 3–7$) are reported here and used in the data analysis.

If nitrite is present in the seawater samples, it can affect detectably the measured nitrate + nitrite $\delta^{18}O$ [*Granger et al*., 2006; *Casciotti et al*., 2007; *Granger and Sigman*, 2009]. We find that this is the case even when nitrite represents as little as ~0.5% of the nitrate + nitrite pool. Because nitrite undergoes a smaller fractional loss of O atoms than nitrate during conversion (3/4 as opposed to 5/6), the N_2O generated from nitrite by the denitrifier method is ~25‰ lower in $\delta^{18}O$ than N_2O generated from nitrate with the same initial $\delta^{18}O$ [*Casciotti et al*., 2007]. Therefore, by calibrating our measured O isotope ratios using nitrate standards, we underestimate the $\delta^{18}O$ of sample nitrate + nitrite. We have corrected the $\delta^{18}O$ for this methodological bias based on the fraction of nitrite (i.e., $[NO_2^-]/[NO_3^- + NO_2^-]$) in each sample. Due to gaps in $[NO_2^-]$ sampling at sea, we apply a constructed $[NO_2^-]$ profile in correcting each $\delta^{18}O$ profile, based on the available $[NO_2^-]$ measurements, World Ocean Circulation Experiment $[NO_2^-]$ data [*Orsi and Whitworth*, 2005] and knowledge of the water column structure (i.e., potential density at each station). For each constructed profile (from the STF southward), $[NO_2^-]$ decreases through the water column (proportionally to increasing potential density) from 0.25 μM at the surface to 0 μM at the base of the pycnocline and is held constant at 0 μM throughout deep waters. It is the corrected $\delta^{18}O$ data that we report throughout this study, with error bars adjusted to account for error propagation.

To investigate the isotopic influence of nitrite on the total nitrate + nitrite pool, nitrite was removed from an aliquot of every seawater sample above 700 m as well as some deeper samples by the addition of sulfamic acid (according to the protocol of *Granger and Sigman* [2009]). The $\delta^{15}N$ and $\delta^{18}O$ of these "nitrate-only" samples were then measured 3 to 7 times for comparison with the nitrate + nitrite data. The pooled sample standard deviation for $\delta^{15}N$ was 0.05‰ and <0.08‰ for more than 90% of the samples ($n = 3–7$), while for $\delta^{18}O$, the pooled sample standard deviation was 0.13‰ and <0.19‰ in 90% of cases ($n = 3–7$). For brevity, we refer to nitrate + nitrite measurements as nitrate measurements throughout this study, except where explicitly dealing with the effects of nitrite removal or the significance of the nitrite pool (sections 3.3 and 4.4).

3. Results

3.1. Hydrographic Context

The wintertime transect between the Antarctic sea ice edge and South Africa encompasses a wide range of oceanic environments, from the colder (<0°C), fresher (<34.2 practical salinity unit (psu)) surface waters of the polar ocean to the warmer (>10°C), and saltier (>35.0 psu) waters of the subtropics. At the time of sampling, surface and subsurface (200 m) temperature and salinity properties place the SACCF at 55.7°S, the PF at 50.3°S, the SAF at 46.4°S, and the STF at 39.7°S–40.9°S (Figure 2). Mixed layer depth generally increases northward from 93–124 m in the PAZ to 108–137 m in the OAZ, to 113–153 m in the Polar Frontal Zone (PFZ, between the PF and the SAF), and to 122–189 m in the SAZ. In the Subtropical Zone (STZ, north of the STF) between 35°S and 40°S, mixed layers range from 55 m to 250 m, with the deeper mixed layers being driven by an Agulhas Ring, typical of the region [*Lutjeharms and van Ballegooyen*, 1988; *Boebel et al*., 2003].

3.2. Wintertime Patterns in the Concentration and Isotopic Composition of Nitrate

3.2.1. From South Africa to the Antarctic Sea Ice

The $\delta^{15}N$ and $\delta^{18}O$ of surface nitrate exhibit strong negative correlations with $[NO_3^-]$ south of the STF (Figure 3). Considering the underway surface data alone, the overall decrease in $[NO_3^-]$ from 27.3 μM at 56.6°S to 9.8 μM near the STF (Figure 3a) is coupled with an increase in $\delta^{15}N$ from 5.2‰ to 8.9‰ (Figure 3b) and in $\delta^{18}O$ from 2.9‰ to 7.0‰ (Figure 3c) ($R^2 = -0.99$ for $\delta^{15}N$ and $\delta^{18}O$). North of the STF, however, these

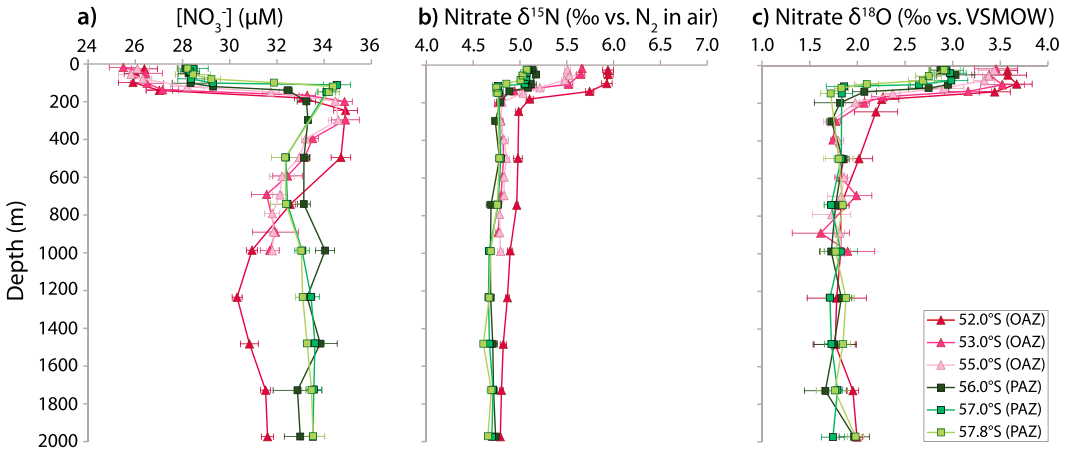

Figure 4. Vertical profiles of (a) [NO_3^-] (in μM), (b) nitrate $\delta^{15}N$ (in ‰ versus N_2 in air), and (c) nitrate $\delta^{18}O$ (in ‰ versus VSMOW) for the upper 2000 m from the wintertime AZ south of Africa, the focus of this study (OAZ in pinks and PAZ in greens; for all 15 profiles from the STZ to the PAZ, see Figure S2 in the supporting information). The error bars indicate the measurement standard deviation ($n \geq 3$).

relationships largely break down, where a further decrease in [NO_3^-] (by ~7.3 μM) is instead accompanied by a sharp decrease in $\delta^{15}N$ and a slight decrease in $\delta^{18}O$ (by ~1.3‰ and ~0.3‰, respectively). This distinct deviation in the $\delta^{15}N$(and $\delta^{18}O$)-to-[NO_3^-] relationship between 35°S and 40°S coincides with warm temperatures (>16°C), high salinities (>35.5 psu), and deep mixed layers (up to 250 m), which are characteristic properties of an Agulhas Ring [*Lutjeharms and van Ballegooyen*, 1988; *Schmid et al*., 2003].

Another dominant pattern in the winter transect is one of decreasing [NO_3^-] toward the surface (Figure 3a), accompanied by rises in $\delta^{15}N$ and $\delta^{18}O$ (Figures 3b and 3c). In terms of the magnitude of these vertical changes, a clear meridional progression is evident, with the smallest deep-to-surface differences in the southernmost PAZ and the greatest deep-to-surface differences in the northernmost SAZ. The degree to which these patterns represent wintertime assimilation or remnant summertime assimilation is investigated for the AZ in section 4.

3.2.2. The Antarctic Zone

Given that spatial and seasonal variations in the N and O isotope patterns of the SAZ have been fairly intensively investigated [*Sigman et al*., 1999; *DiFiore et al*., 2006; *Rafter et al*., 2013], we focus here on the description and analysis of the AZ data (including relevant subsurface water masses). A description of the profile data from the full transect is provided in the supporting information. Quantitative interpretation of the data from north of the AZ will be undertaken in subsequent work [*Smart*, 2014].

In the PAZ, the characteristic subsurface [NO_3^-] maximum of UCDW is evident at 100–200 m with concentrations close to 34 μM, while in the OAZ, maximum concentrations of ~35 μM occur at 200–300 m (Figure 3a and Figure 4a). These maxima roughly correspond with, or fall slightly shallower than, the core potential density (1027.6 kg m^{-3}) of UCDW described elsewhere [*Orsi et al*., 1995; *Sigman et al*., 1999]. The subsurface [NO_3^-] minimum of LCDW is evident at 500–700 m (32–33 μM) in the PAZ deepening northward to 1000–1500 m (30–32 μM) in the OAZ, following or occurring just shallower than the 1027.8 kg m^{-3} isopycnal. LCDW is further distinguished from overlying UCDW by its elevated salinity and higher oxygen content [*Orsi et al*., 1995]. Although their nitrate concentrations differ, UCDW and LCDW are similar in isotopic composition throughout the AZ interior (Figures 3 and 4), with a $\delta^{15}N$ of 4.83 ± 0.07‰ and 4.74 ± 0.07‰, and a $\delta^{18}O$ of 1.89 ± 0.16‰ and 1.81 ± 0.09‰ for UCDW and LCDW, respectively (concentration weighted mean ± standard deviation; $n = 23$ for UCDW and $n = 30$ for LCDW). As the $\delta^{15}N$ elevation of UCDW derives from its exchange with the relatively high $\delta^{15}N$ of Pacific Deep Water [*Rafter et al*., 2013], the weakness of this $\delta^{15}N$ elevation at our section is likely a consequence of it being in the Atlantic sector. The lowest $\delta^{15}N$ (<4.75‰) values are observed in the deepest, most polar waters sampled (south of the SACCF; Figure 3b). Overall, the mean $\delta^{15}N$ and $\delta^{18}O$ of nitrate in the AZ interior are 4.78 ± 0.08‰ and 1.84 ± 0.13‰, respectively ($n = 53$).

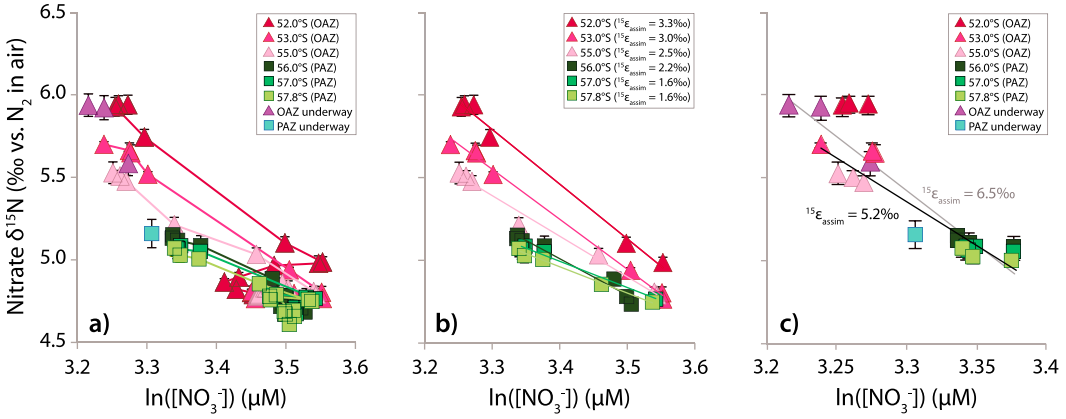

Figure 5. Wintertime data from the OAZ (pink shades) and PAZ (green shades) plotted in nitrate $\delta^{15}N$ versus ln($[NO_3^-]$) space for (a) full AZ vertical depth profiles (and underway surface data) and (b) samples from the surface to the depth of the $[NO_3^-]$ maximum of CDW. The N isotope effect estimates ($^{15}\varepsilon_{assim}$) indicated on the plot for each station derive from the slopes of the linear trendlines. (c) Intercomparison of all AZ mixed layer data (note the change of *x* axis scale for Figure 5c) yielding an $^{15}\varepsilon_{assim}$ estimate of 6.5‰ (grey trendline). Excluding mixed layer samples from the profile at 52.0°S (and nearby underway samples), which appear to derive from a different subsurface source, decreases the slope ($^{15}\varepsilon_{assim}$) to 5.2‰ (black trendline). The discrepancy between depth profile- and mixed layer-based estimates of $^{15}\varepsilon_{assim}$ are consistent with nitrification of low-$\delta^{15}N$ N in the AZ mixed layer.

The PAZ profiles exhibit the smallest vertical changes from the subsurface $[NO_3^-]$ maximum into the mixed layer; $[NO_3^-]$ decreases by 4.8–5.9 μM (Figure 4a) and $\delta^{15}N$ and $\delta^{18}O$ increase by 0.3–0.4‰ and 0.9–1.2‰ (Figures 4b and 4c), respectively. In the OAZ, a $[NO_3^-]$ decrease of 8.5–8.8 μM from the $[NO_3^-]$ maximum into the mixed layer is accompanied by rises in $\delta^{15}N$ and $\delta^{18}O$ of 0.7–1.0‰ and 1.4–1.7‰, respectively.

Plotting the AZ profile data in Rayleigh space (i.e., $\delta^{15}N$ or $\delta^{18}O$ versus ln($[NO_3^-]$)), which assumes closed-system nitrate isotope dynamics) reveals the general trend that is expected from nitrate assimilation by phytoplankton [*Sigman et al.*, 1999; *Altabet and François*, 1994b; *Altabet and François*, 2001; *DiFiore et al.*, 2009], with the OAZ profiles exhibiting a greater degree of consumption (and thus $\delta^{15}N$ and $\delta^{18}O$ elevation) toward the surface than do the PAZ profiles (Figure 5a and Figure 6a).

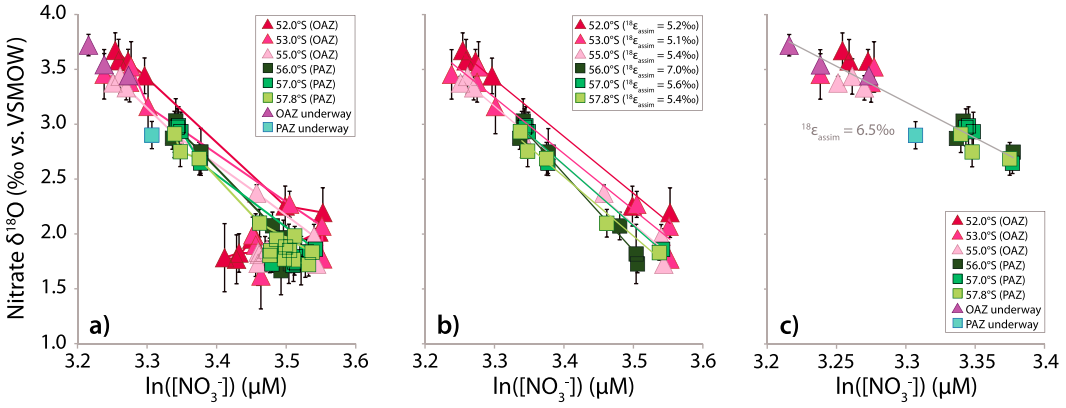

Figure 6. Wintertime data from the OAZ (pink shades) and PAZ (green shades) plotted in nitrate $\delta^{18}O$ versus ln($[NO_3^-]$) space for (a) full AZ vertical depth profiles (and underway surface data) and (b) samples from the surface to the depth of the $[NO_3^-]$ maximum of CDW. The O isotope effect estimates ($^{18}\varepsilon_{assim}$) indicated on the plot for each station derive from the slopes of the linear trendlines. (c) Intercomparison of all AZ mixed layer data (note the change of *x* axis scale for Figure 6c) yielding an $^{18}\varepsilon_{assim}$ estimate of 6.5‰ (grey trendline). Both depth profile- and mixed layer-based estimates of the nitrate assimilation isotope effect from $\delta^{18}O$ data are considerably higher than inferred from the depth profile $\delta^{15}N$ data (Figure 5b), hinting at the decoupling of the N and O isotopes in the upper water column of the AZ.

However, the slopes of the Rayleigh-space $\delta^{15}N$ trends are notably lower than observed from prior measurements of summertime samples from the AZ (the prior data to be described in section 4). Using data down to the $[NO_3^-]$ maximum and thus assuming an UCDW source, these trends yield $^{15}\varepsilon_{assim}$ estimates of 1.6–2.2‰ in the PAZ and 2.5–3.3‰ in the OAZ (Figure 5b). If the upper AZ was an open or steady state system, with continual resupply of nitrate to balance N losses to consumption and export [*Sigman et al*., 1999; *Hayes*, 2002], upper ocean nitrate $\delta^{15}N$ would be better described by the steady state model:

$$\delta^{15}N_{reactant} = \delta^{15}N_{initial} + {}^{15}\varepsilon_{assim} \cdot (1 - f) \quad (2)$$

Analyzing the same $\delta^{15}N$ profiles in the context of the steady state model yields only slightly higher $^{15}\varepsilon_{assim}$ estimates of 1.7–2.4‰ in the PAZ and 2.8–3.8‰ in the OAZ (not shown). The $^{18}\varepsilon_{assim}$ values implied by the AZ $\delta^{18}O$ profile slopes in Rayleigh space (Figure 6b) are all notably higher than the $^{15}\varepsilon_{assim}$ estimates suggested by the $\delta^{15}N$ profiles and fall within a smaller range of 5.1–5.6‰ (with the exception of one station at 56.0°S that suggests an $^{18}\varepsilon_{assim}$ of 7.0‰). The steady state model yields still higher $^{18}\varepsilon_{assim}$ estimates of 5.9–6.2‰ (and 7.6‰ at 56.0°S) (not shown).

In principle, isolating and running a statistical regression through only the mixed layer data from the AZ (in Rayleigh or steady state space) should yield additional estimates of the assimilation isotope effect [*Sigman et al*., 1999], provided that all these mixed layer samples derive from the same deep nitrate source (or different nitrate sources that have the same $\delta^{15}N$- or $\delta^{18}O$-to-$[NO_3^-]$ relationship). Applying this approach to our N isotope data yields an $^{15}\varepsilon_{assim}$ estimate of 6.5‰ in the context of the Rayleigh model (Figure 5c), much higher than derived from the depth profile regressions. Deeper measurements suggest that the particularly high $\delta^{15}N$ of mixed layer nitrate in the northernmost AZ profile at 52.0°S stems from a higher $\delta^{15}N$ for its subsurface nitrate source (by ~0.2‰; see Figure 5a for profile). Excluding mixed layer data from this station and nearby underway samples produces a Rayleigh-based $^{15}\varepsilon_{assim}$ estimate of 5.2‰ for the AZ mixed layer, which is still 1.9–3.6‰ higher than those derived from the profiles. Running a regression line through only the mixed layer $\delta^{18}O$ data in Rayleigh space yields an $^{18}\varepsilon_{assim}$ of 6.5‰ (Figure 6c). This estimate for $^{18}\varepsilon_{assim}$ is within the total range of the profile-based estimates but 0.9‰ higher than the average. It is also notably similar to the $^{15}\varepsilon_{assim}$ estimate from mixed layer data alone.

3.3. The Effect of Nitrite Removal on Antarctic Zone Samples

Onboard measurements of $[NO_2^-]$ indicate deep (>200 m) concentrations of less than 0.1 μM (<0.5% of the $[NO_3^- + NO_2^-]$ pool) and mixed layer concentrations that typically ranged from 0.2 μM to 0.3 μM (0.75–3.0% of the $[NO_3^- + NO_2^-]$ pool) across most of the transect (including the AZ). Despite its relatively small contribution to the total $[NO_3^- + NO_2^-]$ pool, the removal of the nitrite from AZ mixed layer samples yields a higher average $\delta^{15}N$ and $\delta^{18}O$ for nitrate-only relative to untreated samples, by 0.27‰ (Figure S3a in the supporting information) and 0.11‰ (not shown), respectively.

Plotting the nitrate-only N isotope profile data from the AZ in Rayleigh space ($\delta^{15}N$ versus $\ln([NO_3^-])$) yields steeper slopes (and thus higher $^{15}\varepsilon_{assim}$ estimates) than the original nitrate + nitrite data (Figure S3b in the supporting information). The slopes of the PAZ profiles increase from 1.6–2.2‰ to 2.7–3.7‰, while the slopes of the OAZ profiles increase from 2.5–3.3‰ to 3.2–4.0‰. A Rayleigh analysis of nitrate-only mixed layer samples also yields a higher $^{15}\varepsilon_{assim}$ estimate than for nitrate + nitrite (5.8‰ compared to 5.2‰, both excluding the northernmost AZ samples; Figure S3c in the supporting information). In terms of the O isotopes, however, most AZ profile slopes do not change substantially when nitrite is removed, producing $^{18}\varepsilon_{assim}$ estimates of 5.0–6.4‰ for nitrate-only (not shown) compared to 5.1–7.0‰ for nitrate + nitrite. Mixed layer-based estimates of $^{18}\varepsilon_{assim}$ are also similar with and without nitrite removed (6.6‰ (not shown) and 6.5‰, respectively).

4. Discussion

The clear negative correlation that we observe between the nitrate isotopes ($\delta^{15}N$ and $\delta^{18}O$) and concentration ($[NO_3^-]$) reflects the dominant effect of assimilation by phytoplankton on nitrate isotope distributions in the Southern Ocean—this is the dominant isotopic signal even in midwinter. Given the deep mixed layers and low insolation during winter, however, it is likely that the observed gradients (from the subsurface into the mixed layer and across the Southern Ocean surface) are largely remnants of summertime assimilation. The

assimilation signal as a summer remnant is supported by a simple mixing calculation which indicates that the deep-to-surface [NO_3^-] decrease in the wintertime AZ is driven primarily by the low [NO_3^-] of the summer mixed layer, the incorporation of which into the winter mixed layer effectively dilutes its concentration. For the summertime AZ, we use a mixed layer depth of 75 m [*Joubert et al.*, 2011; *Thomalla et al.*, 2011; *Swart et al.*, 2012] and a [NO_3^-] of 24 μM, which routine summer sampling shows to be representative of the region (Thomalla et al., unpublished data, 2008–2014; Fawcett et al., unpublished data, 2014). Deepening a summer mixed layer with these properties to 116 m (the average AZ mixed layer depth observed during the winter cruise) by mixing with underlying UCDW (with a [NO_3^-] of 33.5 μM) would yield a winter mixed layer with a [NO_3^-] of 27.4 μM; this prediction is very close to the observed average [NO_3^-] of 27.3 μM for the wintertime AZ mixed layer.

One might expect therefore that the isotopic elevation of nitrate in wintertime surface waters (compared to deep values) as well as the northward increase in nitrate $\delta^{15}N$ and $\delta^{18}O$ across the region (with increasing consumption) are also largely relics of summertime nitrate assimilation patterns. However, as we describe below, deviations from the typical summertime isotope-to-concentration and N-to-O isotope relationships are observed in the wintertime data reported here, and these deviations indicate additional wintertime processes.

4.1. Anomalously Low Isotope Effect Estimates From Wintertime Antarctic $\delta^{15}N$ Profiles

The $^{15}\varepsilon_{assim}$ estimates of 1.6–3.3‰ yielded by the Rayleigh model analysis of the winter AZ depth profiles (Figure 5b) are remarkably low compared to those suggested by culture studies and summertime data from the AZ. Although the full range of $^{15}\varepsilon_{assim}$ suggested by culture experiments is large (0–20‰ [*Wada and Hattori*, 1978; *Montoya and McCarthy*, 1995; *Granger et al.*, 2004]), most of the data indicate a mean value near 5–6‰ for diatoms [*Waser et al.*, 1998; *Needoba et al.*, 2003; *Needoba and Harrison*, 2004; *Needoba et al.*, 2004; *Granger et al.*, 2010], which are likely to be important for nitrate assimilation in the AZ. Field estimates from the summertime AZ range from as low as 4‰ to as high as 10‰, but the evidence for persistent isotope effects lower than 5‰ is weak [*Sigman et al.*, 1999; *Altabet and François*, 2001; *Karsh et al.*, 2003; *DiFiore et al.*, 2009]. An $^{15}\varepsilon_{assim}$ of 1.5–3‰ can be ruled out for the summertime Southern Ocean [*Sigman et al.*, 1999; *Karsh et al.*, 2003; *DiFiore et al.*, 2009] as well as for the summertime North Pacific and other regions [e.g., *Wu et al.*, 1997; *Altabet et al.*, 1999; *Altabet*, 2001; *Yoshikawa et al.*, 2006; *Brunelle*, 2009]. Using a linear model approach in *R*, we find that our mean $^{15}\varepsilon_{assim}$ estimates for both the OAZ (3.0 ± 0.28‰) and PAZ (1.8 ± 0.13‰) are significantly different from an $^{15}\varepsilon_{assim}$ of 5‰ (at the lower range of summertime AZ estimates), with $P < 0.001$ in both cases. Given that much of the signal in the wintertime AZ should be a remnant of the summertime nitrate drawdown signal, such low $^{15}\varepsilon_{assim}$ estimates are particularly surprising. Furthermore, any wintertime assimilation overlain on this remnant summertime signal is more likely to raise (rather than lower) the estimated $^{15}\varepsilon_{assim}$, due to the deeper mixed layers and lower daily insolation experienced during winter [*Needoba and Harrison*, 2004; *DiFiore et al.*, 2010]. Under such conditions, phytoplankton appear to efflux proportionally more of the isotopically elevated intracellular nitrate into the environment, resulting in a larger expressed isotope effect [*Needoba et al.*, 2004; *Needoba and Harrison*, 2004; *Karsh*, 2013].

A suspicion that one might have is that the anomalously low $\delta^{15}N$ versus ln([NO_3^-]) slopes of the AZ depth profiles derive from the inappropriateness of the Rayleigh model for the interpretation of winter data. Specifically, nitrate consumption in the absence of new nitrate supply is clearly inconsistent with deep wintertime mixing. Recalculating these slopes using a model that includes continuous mixing between the winter mixed layer and water below it (the opposite end-member case, the steady state model), however, does not significantly increase the $^{15}\varepsilon_{assim}$ implied by the data (1.7–3.8‰; not shown). The lack of difference derives from the insensitivity of the Rayleigh model to nitrate resupply at low degrees of consumption [*Sigman et al.*, 1999]. Under the low nitrate utilization levels of the wintertime AZ (<30%), surface and deep water masses are not different enough in [NO_3^-] and $\delta^{15}N$ for their mixing to produce a deviation from a pure utilization trend that is sufficiently large to explain our data.

An alternative dynamic that could be responsible for lowering the net wintertime isotope effect involves phytoplankton growth within sea ice. When nitrate assimilation takes place in sea ice, consumption proceeds to high degrees within the ice structure, causing incomplete expression of the organism-level assimilation isotope effect and thus a low net isotope effect in the water column [*Fripiat et al.*, 2014]. If this was the reason for the low isotope effects suggested by our $\delta^{15}N$ profiles, however, we would expect to observe the

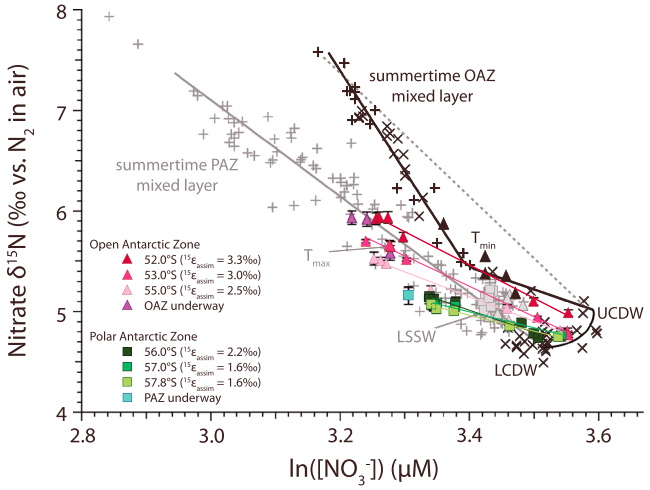

Figure 7. Comparison of our winter nitrate δ^{15}N data from the AZ south of Africa (OAZ in pink and PAZ in green; profiles extending down to the [NO_3^-] maximum of CDW at each station) with the Indo-Pacific AZ data shown in Figure 1 [*DiFiore et al.*, 2010]. The anomalously low slopes of our AZ profiles are reminiscent of those connecting UCDW with the summer T_{min} in the data from the Australian sector.

same effect in the δ^{18}O profiles, which is not the case (see below). Another strong argument against this explanation for the low winter AZ δ^{15}N versus ln([NO_3^-]) slopes is provided by the Rayleigh model analysis of the AZ mixed layer data alone (Figure 5c). The regression line slope in Figure 5c implies an $^{15}\varepsilon_{assim}$ of 5.2‰ for the AZ mixed layer, higher than the estimates derived from the δ^{15}N profile data (Figure 5b) and in much better agreement with the summertime estimates from the AZ. The disagreement between the mixed layer- and depth profile-based $^{15}\varepsilon_{assim}$ estimates is consistent with an additional process, operating over multiple years, modifying the CDW-to-winter mixed layer gradient and thus compromising its use as an accurate measure of $^{15}\varepsilon_{assim}$.

As described above, *Sigman et al.* [1999] found the T_{min} layer of summertime profiles from the Indian and Pacific sectors to be a low-δ^{15}N anomaly (kink) in Rayleigh space, falling well below the expected utilization trend between underlying UCDW and the mixed layer (Figure 1). The low slopes connecting UCDW with the T_{min} layer in those summer profiles are thus analogous to our wintertime UCDW-to-mixed layer slopes. *DiFiore et al.* [2010] proposed that the influence of low-δ^{15}N LCDW, via lateral exchange between the T_{min} and T_{max} layers (the latter of which is fed by LCDW from below), was responsible for the anomalous character of the T_{min}. However, intrusion of LCDW nitrate into the T_{min} layer cannot explain the low slopes of the Atlantic AZ winter profile data reported here. The failure of this explanation derives from the greater similarity between UCDW and LCDW [NO_3^-] and δ^{15}N in the Atlantic sector AZ, rendering them almost indistinguishable as nitrate sources (Figure 7). This leads us to seek an alternative to the hydrographic explanation of *DiFiore et al.* [2010] to account for the lowering of nitrate δ^{15}N in the winter mixed layer and thus explain the unexpectedly low $^{15}\varepsilon_{assim}$ implied by our AZ δ^{15}N profiles.

4.2. Decoupling of the N and O Isotopes as Evidence for Mixed Layer Nitrification

Culture studies have shown that nitrate assimilation produces roughly equal elevations in the δ^{15}N and δ^{18}O of nitrate, such that $^{15}\varepsilon_{assim}$ is approximately equal to $^{18}\varepsilon_{assim}$ [*Granger et al.*, 2004, 2010]. Thus, if the only biological process acting upon nitrate in the AZ profiles was assimilation, we would expect all the data to fall along a 1:1 line in δ^{18}O versus δ^{15}N space, extending from the average δ^{18}O and δ^{15}N of the deep nitrate source. However, as we trace the AZ profiles from their deep source into the winter mixed layer, there is a clear deviation above the 1:1 line, with a rise in δ^{18}O that is roughly double to triple the rise in δ^{15}N (Figure 8a).

This type of deviation from 1:1 argues for partial nitrate assimilation coupled with in situ nitrification in the AZ winter mixed layer. Suspended particulate nitrogen (PN) produced in the AZ surface is low in δ^{15}N due to the modest degree of nitrate utilization that occurs in this region [*Sigman et al.*, 1999, 2009c] as well as other processes in the upper ocean N cycle described below. When this PN is remineralized and nitrified, its low-δ^{15}N signal is preserved in the resulting nitrate, while the δ^{18}O of the nitrate is reset to the nitrification value (estimated to be ~1.1‰ higher than ambient water by *Sigman et al.* [2009c]; see also *Buchwald et al.* [2012]). Because the regenerated nitrate has a combined δ^{18}O and δ^{15}N that lies above the 1:1 line (the point toward which the blue dashed lines project in Figure 8a; see caption for details), its addition to the partially assimilated mixed layer nitrate lowers the δ^{18}O of the resultant nitrate pool less than it lowers the δ^{15}N, driving the mixed layer samples off the 1:1 line (in the direction indicated by the blue arrows in Figure 8a).

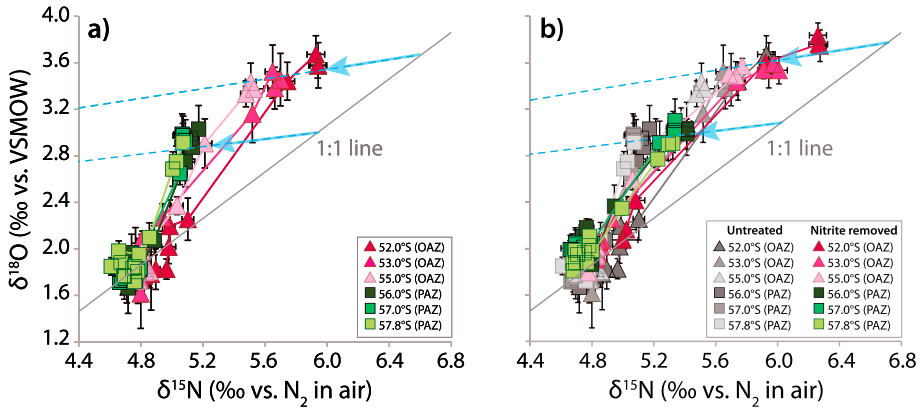

Figure 8. Wintertime AZ depth profiles in $\delta^{18}O$ versus $\delta^{15}N$ space showing (a) the untreated samples (i.e., nitrate + nitrite; OAZ in pink and PAZ in green) and (b) a comparison between untreated samples (in grey) and the same samples with nitrite removed (i.e., nitrate only; OAZ in pink and PAZ in green). A solid grey 1:1 line passes through the average $\delta^{18}O$ and $\delta^{15}N$ of the deep nitrate source (assumed to be CDW), illustrating the trajectory that the profiles would follow if the only process occurring in the mixed layer was nitrate assimilation. The blue arrows schematically show the effect of in situ nitrification on AZ mixed layer samples in this space. The blue dashed lines project through the average measured $\delta^{18}O$ and $\delta^{15}N$ of mixed layer nitrate (either OAZ or PAZ) toward the approximate $\delta^{18}O$ and $\delta^{15}N$ expected for newly nitrified nitrate (1.1‰ and −5.8‰, respectively, the latter being the approximate $\delta^{15}N$ of PN in late summer/autumn that is required for its regeneration to explain the low $\delta^{15}N$ versus $\ln([NO_3^-])$ slopes in Figure 5b). The vertical and horizontal error bars represent the standard deviation of $\delta^{18}O$ and $\delta^{15}N$ measurements, respectively.

The decoupling of the N and O isotopes by nitrification is likely responsible for some of the differences between the $\delta^{15}N$ and $\delta^{18}O$ gradients observed in the wintertime AZ. For instance, the significantly greater range in $\delta^{15}N$ versus $\ln([NO_3^-])$ slopes across the AZ (which increase from south to north) relative to the $\delta^{18}O$ versus $\ln([NO_3^-])$ slopes from the same profiles (compare Figure 5b with Figure 6b) likely reflects the greater proportional importance of the nitrification signal to the south where the nitrate assimilation signal is weaker. In addition, regenerated nitrate $\delta^{15}N$ will be sensitive to the $\delta^{15}N$ of the PN being regenerated, with lower-$\delta^{15}N$ PN being produced at higher latitudes due to a lower degree of nitrate consumption.

The offset between mixed layer- and profile-based estimates of the isotope effect, in the case of both N and O, is likely a result of the different time scales recorded by lateral versus vertical gradients. The mixed layer sample sets capture the assimilation-driven meridional gradient in nitrate isotopes, which is erased by lateral exchange of surface waters on a time scale of less than a year. In contrast, the vertical gradients in nitrate isotopes integrate over periods longer than a year, as it takes years for mixed layer nitrate to be replaced by exchange with underlying deepwater nitrate. The larger offset between mixed layer- and profile-based isotope effect estimates for N than for O may be another manifestation of the decoupling effect of nitrification. Nitrification in the mixed layer would act to dampen the assimilation signal in both the N and O isotope profiles (producing lower apparent isotope effects) but more so for N since the $\delta^{15}N$ of ambient nitrate is lowered more by in situ nitrification than is its $\delta^{18}O$.

4.3. Summer-to-Autumn Decline in Suspended PN $\delta^{15}N$

Above, we argue that the low $\delta^{15}N$ of nitrate in the winter mixed layer of the AZ south of South Africa is best explained as the result of the regeneration/nitrification of low-$\delta^{15}N$ suspended PN, with the coupled N and O isotope measurements of the winter mixed layer offering supporting evidence. However, a lower $\delta^{15}N$ for newly nitrified nitrate is needed to generate the very low $\delta^{15}N$ versus $\ln([NO_3^-])$ slopes of the wintertime AZ profiles (and the T_{min} kink observed in summertime profiles; Figure 7) than is needed to cause the observed deviation from 1:1 in $\delta^{18}O$ versus $\delta^{15}N$ space (Figure 8a). To drive a deviation from 1:1, the $\delta^{15}N$ of newly nitrified nitrate can theoretically be any value less than 4.1‰. This is because newly nitrified nitrate with a $\delta^{18}O$ of 1.1‰ [*Sigman et al.*, 2009c] would need to have a $\delta^{15}N$ of 4.1‰ to fall on the 1:1 line. Any lower $\delta^{15}N$ value would cause a deviation above the 1:1 line. However, to lower nitrate $\delta^{15}N$ to the values observed in the wintertime mixed layer, the $\delta^{15}N$ of newly nitrified nitrate must be much lower than 4.1‰.

To provide a quantitative estimate for the required $\delta^{15}N$ of newly nitrified nitrate, we consider the AZ winter mixed layer to have four different nitrate sources: (1) the previous summer mixed layer in this region,

with a $\delta^{15}N$ of 6.3‰ and [NO_3^-] of 24.1 μM (Fawcett et al., unpublished data, 2014) and a thickness of 75 m [*Joubert et al*., 2011; *Thomalla et al*., 2011; *Swart et al*., 2012]; (2) the previous summer T_{min}, with a $\delta^{15}N$ of 5.4‰ and [NO_3^-] of 27.3 μM (using our average AZ winter mixed layer properties as a proxy) and a thickness of 41 m (taken from the difference between average winter and summer mixed layer depths); (3) newly nitrified nitrate, assuming complete regeneration of the summertime AZ suspended PN pool, with an average [PN] of 1.3 μM (Fawcett et al., unpublished data, 2014); and (4) UCDW, with a $\delta^{15}N$ of 4.8‰ and [NO_3^-] of 33.5 μM. In principle, in order to reproduce the average observed properties of the AZ winter mixed layer ($\delta^{15}N$ of 5.4‰ and [NO_3^-] of 27.3 μM) from this combination of sources, UCDW would need to contribute 0.8 μM of nitrate through upwelling and vertical mixing between summer and winter sampling. With these combined constraints, we calculate that the $\delta^{15}N$ of the regenerated PN would theoretically need to be −5.8‰. Such a $\delta^{15}N$ for PN is lower than can be achieved by fractionation during nitrate assimilation alone.

Based on the abundant early to midsummer data for the $\delta^{15}N$ of AZ mixed layer PN, the $\delta^{15}N$ of suspended PN appears to have a mean near 0‰ [*Altabet and François*, 1994a; *Altabet and François*, 2001; *Lourey et al*., 2003; *DiFiore et al*., 2009]. This value is not adequately low for its regeneration/nitrification to explain the low $\delta^{15}N$ of nitrate in the winter mixed layer and summertime T_{min}. However, starting in January/February in the AZ south of Australia, *Lourey et al*. [2003] observe a substantial drop in suspended PN $\delta^{15}N$ to ~−5‰ in March. This low-$\delta^{15}N$ PN can apparently explain the very low $\delta^{15}N$ versus ln([NO_3^-]) slopes of the wintertime AZ profiles and thus the amplitude of the $\delta^{15}N$ kink in the summertime T_{min}.

This then raises the question of why suspended PN $\delta^{15}N$ would decline so strongly from summer to autumn in the AZ. This change appears to overlap with the spring/summer period during which nitrate $\delta^{15}N$ is rising due to nitrate consumption and thus when nitrate assimilation should be causing particle $\delta^{15}N$ to rise. In light of observations from the subtropics [*Altabet*, 1988; *Fawcett et al*., 2011, 2014], it is logical to suspect that the $\delta^{15}N$ decline reflects an increase in the assimilation of regenerated N (in particular, ammonium). Ammonium is low in $\delta^{15}N$ relative to nitrate (the alternative source), due to net isotope fractionation (estimated to be around 3‰) during bacterial degradation of particulate organic matter [*Lehmann et al*., 2002] and metabolism and excretion of ammonium by zooplankton [*Checkley and Miller*, 1989]. These effects may be compounded by continued remineralization of PN as it sinks: as with heterotrophic degradation of suspended particles [*Altabet and McCarthy*, 1986], fractionation during remineralization of sinking particles would cause sinking PN to export relatively high $\delta^{15}N$ material from the mixed layer [*Möbius*, 2013], further lowering the $\delta^{15}N$ of ammonium available for assimilation within the mixed layer in late summer. By the end of the productive season (i.e., autumn), the PN remaining in surface waters would be low in $\delta^{15}N$ which, once remineralized and nitrified in the wintertime mixed layer, could lower the $\delta^{15}N$ of the ambient nitrate beyond Rayleigh or steady state predictions. In order to verify these explanations and improve our understanding of upper ocean N cycling in the AZ, greater seasonal and spatial coverage of PN $\delta^{15}N$ measurements is needed, particularly for late summer and autumn.

4.4. The Isotopic Influence of Nitrite in the Antarctic Winter Mixed Layer

In early studies of Antarctic nitrate, no attempt was made to correct for the presence of nitrite on the grounds of low ambient concentrations [e.g., *Sigman et al*., 1999; *DiFiore et al*., 2009]. The results of our nitrite-removal tests, however, reveal that the small quantity of nitrite in our AZ mixed layer samples (0.2–0.3 μM) lowers the $\delta^{15}N$ and $\delta^{18}O$ of the nitrate + nitrite measurably by an average of 0.27‰ and 0.11‰, respectively.

The $\delta^{18}O$ effect is relatively complex, involving both the $\delta^{18}O$ of ambient nitrite and the equilibration of nitrite with seawater after sample collection [*Casciotti et al*., 2007; *Buchwald and Casciotti*, 2013]. However, the $\delta^{15}N$ effect simply reflects what must be a very low $\delta^{15}N$ for the ambient nitrite; mass balance calculations imply a $\delta^{15}N$ of −40‰ to −20‰ to be typical for AZ mixed layer nitrite (−30‰ on average based on our constructed [NO_2^-] profiles and −29‰ based on shipboard [NO_2^-] data). These values are in line with the measured N isotope effects of ammonium oxidation (14–19‰ [*Casciotti et al*., 2003]) and nitrite oxidation (−12.8‰ [*Casciotti*, 2009]).

If we assume a $\delta^{15}N$ range of −3‰ to 0‰ for ammonium (based on the commonly observed value of 0‰ for suspended PN $\delta^{15}N$ in AZ surface waters [*Altabet and François*, 1994a; *Altabet and François*, 2001; *Lourey et al*., 2003; *DiFiore et al*., 2009] and a remineralization isotope effect of 3‰ [*Lehmann et al*., 2002]), the range of possible $\delta^{15}N$ values for a nitrite pool undergoing simultaneous production (via ammonium

oxidation) and consumption (via nitrite oxidation) is −34.8‰ to −14‰. This picture could be complicated by the concurrent direct assimilation of ammonium by phytoplankton, which would probably act to lower the $\delta^{15}N$ of the ambient nitrite pool, or concurrent assimilation of nitrite by phytoplankton, which would probably act to raise the $\delta^{15}N$ of the ambient nitrite pool [*DiFiore et al*., 2009]. Nonetheless, the extremely low $\delta^{15}N$ of nitrite implied by our measurements cannot be explained solely by efflux of nitrite from phytoplankton cells during nitrate reduction, which would have a $\delta^{15}N$ on the order of −2‰ (based on the nitrate uptake, efflux, and reduction isotope effects of *Karsh* [2013]; see supporting information). Thus, the very low $\delta^{15}N$ reconstructed for winter mixed layer nitrite is additional compelling evidence for nitrite production and oxidation in the AZ winter mixed layer.

Considering the effect of nitrite removal in Rayleigh space, the $^{15}\varepsilon_{assim}$ estimates yielded by the nitrate-only winter AZ profiles are not as anomalously low as those implied by the original nitrate + nitrite data (Figure S3b in the supporting information) but are still lower than commonly observed in the summertime AZ (i.e., slopes in Rayleigh space imply $^{15}\varepsilon_{assim} \leq 4‰$). Moreover, nitrite removal does not appear to drastically alter the $\delta^{18}O$-to-$\delta^{15}N$ relationship in the winter mixed layer; a clear deviation above the 1:1 line remains (Figure 8b). Given the low $\delta^{15}N$ for nitrite (which is consistent with regeneration adding low-$\delta^{15}N$ N back into the nitrate pool, with part of this N being captured as nitrite during the wintertime sampling), the combined winter nitrate + nitrite pool (rather than the winter nitrate-only pool) is arguably the best measure of the $\delta^{15}N$ of nitrate that will be supplied to phytoplankton in the spring. In any case, the evidence and arguments for wintertime nitrification as the driver of the lower-than-expected nitrate (nitrate + nitrite or nitrate-only) $\delta^{15}N$ are not contingent on the question of whether nitrite should be included as a pool that will eventually be incorporated into the spring/summer nitrate pool.

4.5. Implications

4.5.1. Significance and Origin of the T_{min} Anomaly

The anomalously low $\delta^{15}N$ of the T_{min} layer has complicated estimation of $^{15}\varepsilon_{assim}$ in the AZ [*Sigman et al*., 1999; *Karsh et al*., 2003; *DiFiore et al*., 2010]. In the absence of winter data, *Sigman et al*. [1999] assumed that UCDW was the ultimate nitrate source to the summertime surface, yielding $^{15}\varepsilon_{assim}$ estimates in the 4–6‰ range for the OAZ. The isotope and concentration gradients that we observe from the subsurface into the AZ winter mixed layer (Figure 4), however, imply that wintertime mixing is not adequately deep or vigorous to reset the AZ surface to deep source (e.g., UCDW) values. Rather, our data agree better with those of *DiFiore et al*. [2010], suggesting that the T_{min} layer, or ideally the winter mixed layer itself (which lacks any of the summertime modification of the T_{min}), is the ultimate nitrate source to the summer AZ surface. Using the $[NO_3^-]$ and $\delta^{15}N$ of the winter mixed layer (rather than those of UCDW) as an approximation for the starting point of summertime nitrate assimilation yields $^{15}\varepsilon_{assim}$ values ~1.2‰ higher than those estimated initially by *Sigman et al*. [1999] for OAZ profiles from south of Australia [*DiFiore et al*., 2010].

Although our winter data and those of *DiFiore et al*. [2010] are in agreement over a T_{min} source to the spring/summer AZ surface, they differ in their attribution of its low $\delta^{15}N$. While *DiFiore et al*. [2010] call upon the intrusion of low-$\delta^{15}N$ LCDW-sourced nitrate from the south (via T_{max}-T_{min} exchange), our data suggest the wintertime modification of UCDW nitrate (supplied from below by mixing and upwelling) by in situ regeneration/nitrification of low-$\delta^{15}N$ PN within the mixed layer. Thus, a major distinction between the two explanations is that they call for different ultimate nitrate sources to the upper AZ: LCDW versus UCDW.

One way to distinguish between these explanations is to compare the $\delta^{15}N$ of the long-term (i.e., annual) export predicted by each scenario with sediment trap and other field measurements from the AZ. We undertake this test with nitrate isotope data from the AZ south of Australia [*DiFiore et al*., 2010] due to the availability of sediment trap data from the same region. Combining the summer mixed layer and T_{min} layer data, we calculate that the summertime AZ upper water column (down to the base of the T_{min}) has a nitrate $\delta^{15}N$ of ~5.8‰ and a $[NO_3^-]$ of ~29.4 μM. If LCDW (with a $\delta^{15}N$ of 4.8‰ and $[NO_3^-]$ of 33 μM) is the sole nitrate source, a simple mass balance calculation suggests that the $\delta^{15}N$ of the nitrate that would need to be removed (and thus the $\delta^{15}N$ of the PN exported) to produce this combination of summertime conditions is ~−3.3‰. The same calculation with UCDW as the sole nitrate source (with a $\delta^{15}N$ of 5.3‰ and $[NO_3^-]$ of 35 μM), on the other hand, yields a predicted $\delta^{15}N$ of ~+2.8‰ for the sinking PN flux. Deepwater sediment traps from across the PFZ and AZ (54°S–66°S) south of Australia (140°E) and New Zealand (170°E) (nine in total between 830 m and 4224 m, with sampling durations of 7 to 17 months) indicate a $\delta^{15}N$ range of

−1‰ to 5‰ for sinking PN [*Altabet and François*, 2001; *Lourey et al*., 2003]. When only AZ traps that sample a full year are considered (two traps, one from the OAZ and one from the PAZ), the mean flux-weighted δ^{15}N of sinking PN is 0.8‰ [*Altabet and François*, 2001]. These data call for a greater proportion of the AZ nitrate supply to derive from UCDW (around 60–70%) and are therefore consistent with our wintertime nitrification explanation for the T_{min} anomaly. Lateral nitrate exchange (as per *DiFiore et al*. [2010]) may still play a significant role in the low δ^{15}N of the T_{min} nitrate, but if so, it is secondary to the effect of remineralization.

4.5.2. Active Mixed Layer Nitrification

Active nitrification in the wintertime AZ mixed layer is evident from the decoupling of the N and O isotopes of nitrate in the upper water column of this region. This can complicate the inference of nitrate utilization from paleoceanographic records, as sedimentary δ^{15}N will reflect not only the δ^{15}N of deep-source nitrate (and the isotope effect with which it was assimilated) but also the δ^{15}N of newly nitrified nitrate. We have seen firsthand the potential for nitrification to obscure the manifestation of $^{15}\varepsilon_{assim}$ in mixed layer nitrate δ^{15}N, an effect that could be passed on to the δ^{15}N of PN [*DiFiore et al*., 2009]. That is, the anomalously low δ^{15}N that we observe for mixed layer nitrate translates into a lower δ^{15}N for sinking PN and diatom-microfossil-bound organic N. Consequently, sediments underlying waters that host significant levels of mixed layer nitrification, either today or in the past, might be vulnerable to underestimation of the degree of nitrate consumption in surface waters.

The *f* ratio, defined as the ratio of new production to primary (i.e., new plus regenerated) production, is conventionally used to quantify the strength of the biological pump (the export of organic carbon to the deep ocean via biological production). High *f* ratios suggest an ecosystem supported largely by "new" nutrients from below the euphotic layer (rather than nutrients recycled within surface waters) and generally characterized by substantial export [*Dugdale and Goering*, 1967; *Eppley and Peterson*, 1979]. Traditionally, nitrification was regarded as a subeuphotic zone phenomenon, either due to light inhibition of nitrifying bacteria [*Olson*, 1981], or competition for substrate with ammonium-assimilating phytoplankton [*Ward*, 2005]. Assuming that nitrification is vertically separated from primary production within the water column has led to the use of a simplified form of the *f* ratio, with nitrate uptake as an approximation for new production [*Dugdale and Goering*, 1967; *Eppley and Peterson*, 1979]. If, however, nitrification does occur at significant levels within the euphotic zone, some of the nitrate taken up by phytoplankton is actually regenerated, leading to a decoupling from new production and an overestimation of carbon export [*Yool et al*., 2007].

In their investigation of the summertime coastal PAZ, *DiFiore et al*. [2009] find the N and O isotopes of nitrate to be tightly coupled (with all profiles lying close to the 1:1 line in δ^{18}O versus δ^{15}N space) and interpret this as indicating minimal nitrification ($\leq$6% of the nitrate assimilation rate). The observation that nitrification occurs at significant levels in the AZ surface during winter (this study) but not in summer [*DiFiore et al*., 2009] implies sensitivity to seasonal changes in the Southern Ocean. Two nonexclusive interpretations are possible [*Olson*, 1981; *Ward*, 2005]. First, phytoplankton may be outcompeting nitrifiers for regenerated ammonium in the summer mixed layer, with nitrifiers only consuming a significant fraction of the ammonium in the winter when incident radiation is lower and mixed layers are deep. Second, according to the same considerations regarding sunlight, nitrification may be light inhibited in the summer.

The AZ surface may be conducive to nitrification because of its highly seasonal nature. Unlike the low latitudes (where nitrification is largely confined to waters below the base of the euphotic zone [*Ward*, 2005; *Beman et al*., 2008; *Newell et al*., 2013]), the polar ocean is characterized by both a discrete productive summer period (which supplies the PN for subsequent regeneration to ammonium) and a low-light winter period with deeper mixed layers (which may free nitrifiers from both competition for ammonium and light inhibition). Additionally, the polar oceans have sea ice, which, with its high ammonium concentrations and more diffuse light, has been found to be a favorable host environment for nitrification [*Priscu et al*., 1990; *Riaux-Gobin et al*., 2005; *Fripiat et al*., 2014]. It remains a challenge to quantify the relative importance of light inhibition and competition for ammonium in setting nitrification rates. Recent findings from the sunlit waters of the Northeast Pacific [*Smith et al*., 2014] and Antarctic springtime sea ice [*Fripiat et al*., 2014] suggest that competition with ammonium-assimilating phytoplankton is the dominant control on nitrification in those environments.

In contrast to our findings, the coastal PAZ shows no sign of wintertime nitrification in the upper water column [*DiFiore et al*., 2009]. This region has neither a summertime T_{min} layer nor a substantial decrease in

nitrate concentration into the upper ocean during the winter. Thus, the absence of an upper ocean nitrification signal may be explained by dilution with deep nitrate due to the extremely deep winter mixing that characterizes the coastal PAZ.

5. Conclusions

The nitrate $\delta^{15}N$ and $\delta^{18}O$ data from the July 2012 voyage of the R/V *S.A. Agulhas II* offer a rare glimpse into the wintertime conditions and processes in the Southern Ocean south of Africa. The wintertime patterns revealed by the data suggest that nitrate assimilation by phytoplankton remains a dominant control on the N and O isotope distributions of nitrate in the Southern Ocean through the winter (evident in the strong correlation between nitrate isotopes ($\delta^{15}N$ and $\delta^{18}O$) and concentration ($[NO_3^-]$) from the subsurface into the mixed layer and across the Southern Ocean surface), rather than having its signal overwhelmed by deep wintertime mixing. Although the higher resupply rates relative to uptake during winter prevent us from producing accurate estimates of the isotope effect using the closed-system (Rayleigh) model, analyzing the data within a Rayleigh framework proves useful for identifying and interpreting deviations from the predicted nitrate utilization trend. In particular, the Antarctic winter mixed layer is observed to have an anomalously low $\delta^{15}N$-to-$[NO_3^-]$ relationship in Rayleigh space, similar to that observed previously for the T_{min} layer in summertime depth profiles from the Antarctic. This observation substantiates the claim that the summer T_{min} is more representative of the springtime nitrate source (i.e., the starting point for assimilation) than the underlying UCDW [*DiFiore et al.*, 2010] and thus provides support for a higher summertime isotope effect than initially estimated for the Antarctic under the assumption of an UCDW source [*Sigman et al.*, 1999].

However, the winter data point to an alternative to the previously proposed hydrographic explanation for the T_{min} anomaly. Comparison of the $\delta^{15}N$ and $\delta^{18}O$ gradients of nitrate in Antarctic depth profiles demonstrates the decoupling of the two isotope systems in the upper water column, with $\delta^{15}N$ exhibiting substantially weaker increases from the deep nitrate source into the mixed layer than $\delta^{18}O$. We interpret this decoupling as evidence for significant in situ nitrification within the Antarctic winter mixed layer. In order for nitrification to produce such low $\delta^{15}N$ values for winter mixed layer nitrate (and thus also for the summertime T_{min}), we estimate that the $\delta^{15}N$ of suspended PN available for regeneration must be lower than −5‰. To lower PN $\delta^{15}N$ to this extent, in turn, calls for intensive late summer N recycling in the Antarctic, most likely via a growing reliance of phytoplankton on ammonium (rather than nitrate) toward the end of the productive season. The isotopic influence of nitrite in our samples was surprising given the low ambient concentrations of nitrite (relative to nitrate) and serves to caution against simply dismissing its effect on these grounds alone. Nonetheless, the presence of nitrite in the Antarctic winter mixed layer and its very low $\delta^{15}N$ are consistent with ongoing in situ nitrification.

The existence of significant nitrification in winter (but not in summer) underlines the sensitivity of nitrification to seasonal changes in Antarctic surface waters, whether related to changing light conditions or ammonium availability. In order to accurately estimate the export of organic carbon to the deep ocean based on nitrate uptake rates, one must account for the fraction of the organic N deriving from nitrate uptake that will subsequently be regenerated and nitrified within the Antarctic winter mixed layer. In addition, the $\delta^{15}N$ of the nitrate generated in situ in the Antarctic mixed layer points to a late summer Antarctic ecosystem dominated by ammonium rather than nitrate assimilation, a transition that should offer much insight into the controls on export production in the Antarctic. Finally, the key findings outlined above ((1) clarification of the springtime nitrate source, (2) confirmation of a higher summertime isotope effect for nitrate assimilation, (3) demonstration of wintertime mixed layer nitrification, and (4) implication of an intense late summer ammonium cycle) provide critical baseline information for the use of N isotopes as a paleoceanographic proxy for the degree of nitrate consumption in the Antarctic.

Acknowledgments

The data presented in this study can be found at http://www.bco-dmo.org. Support for this work was provided by the South African National Research Foundation; the Applied Centre for Climate and Earth Systems Science; the University of Cape Town; US NSF grants PLR-1401489, OPP-0612198, OCE-0992345, OCE-1136345, and OCE-1060947 (D.M.S.), by the Grand Challenges Program of Princeton University; as well as the European Commission Seventh Framework Program through the GreenSeas Collaborative Project, FP7-ENV-2010 contract 265294. Sincere thanks to P. Monteiro, without whom this work would not have been possible. We are grateful to the captain and crew of the R/V *S.A. Agulhas II* for a safe wintertime voyage, as well as fellow scientists for the assistance in sampling and auxiliary data collection (particularly R. Roman for onboard nutrient analyses). We thank S. Swart for the collection of summertime samples in February 2014 (SANAE 53); S. Oleynik, GC/IRMS laboratory manager at Princeton University, for providing an efficient and enjoyable working environment; M. Prokopenko and A. Martínez-Garcia for the constructive thesis reviews; as well as P. Rafter, F. Fripiat, and R. Philibert for the helpful discussions. This manuscript benefitted from the inputs of two anonymous reviewers.

References

Altabet, M. (1988), Variations in nitrogen isotopic composition between sinking and suspended particles: Implications for nitrogen cycling and particle transformation in the open ocean, *Deep Sea Res., Part I*, *35*, 535–554, doi:10.1016/0198-0149(88)90130-6.

Altabet, M. (2001), Nitrogen isotopic evidence for micronutrient control of fractional NO_3^- utilization in the equatorial Pacific, *Limnol. Oceanogr.*, *46*(2), 368–380, doi:10.4319/lo.2001.46.2.0368.

Altabet, M., and R. François (1994a), Sedimentary nitrogen isotopic ratio as a recorder for surface ocean nitrate utilization, *Global Biogeochem. Cycles*, *8*(1), 103–116, doi:10.1029/93GB03396.

Altabet, M., and R. François (1994b), The use of nitrogen isotopic ratio for reconstruction of past changes in surface ocean nutrient utilization, *Carbon Cycling in the Glacial Ocean: Constraints on the Ocean's Role in Global Change*, *NATO ASI Ser.*, vol. 17, pp. 281–306, Springer, Berlin.

Altabet, M., and R. François (2001), Nitrogen isotope biogeochemistry of the Antarctic Polar Frontal Zone at 170°W, *Deep Sea Res., Part II*, *48*, 4247–4273, doi:10.1016/S0967-0645(01)00088-1.

Altabet, M., and J. McCarthy (1986), Vertical patterns in ^{15}N natural abundance in PON from the surface waters of warm-core rings, *J. Mar. Res.*, *44*, 185–201, doi:10.1357/002224086788460148.

Altabet, M., C. Pilskaln, R. Thunell, C. Pride, D. Sigman, F. Chavez, and R. François (1999), The nitrogen isotope biogeochemistry of sinking particles from the margin of the eastern North Pacific, *Deep Sea Res., Part I*, *46*, 655–679, doi:10.1016/S0967-0637(98)00084-3.

Ansorge, I. (2012), Monitoring the oceanic flow between Africa and Antarctica: Preliminary report on an early winter transect to study the impacts of seasonality on the Antarctic Circumpolar Current, *VOY03 Cruise Report*, South African Southern Ocean Community (SASOC).

Ansorge, I., S. Speich, J. Lutjeharms, G. Göni, C. Rautenbach, P. Froneman, M. Rouault, and S. Garzoli (2005), Monitoring the oceanic flow between Africa and Antarctica: Report of the first GoodHope cruise, *S. Afr. J. Sci.*, *101*, 29–35.

Belkin, I., and A. Gordon (1996), Southern Ocean fronts from the Greenwich meridian to Tasmania, *J. Geophys. Res.*, *101*(C2), 3675–3696, doi:10.1029/95JC02750.

Beman, J., B. Popp, and C. Francis (2008), Molecular and biogeochemical evidence for ammonia oxidation by marine Crenarchaeota in the Gulf of California, *Int. Soc. Microb. Ecol. J.*, *2*, 429–441, doi:10.1038/ismej.2007.118.

Bindoff, N., M. Rosenberg, and M. Warner (2000), On the circulation and water masses over the Antarctic continental slope and rise between 80 and 150°E, *Deep Sea Res., Part II*, *47*, 2299–2326, doi:10.1016/S0967-0645(00)00038-2.

Boebel, O., J. Lutjeharms, C. Schmid, W. Zenk, T. Rossby, and C. Barron (2003), The Cape Cauldron: A regime of turbulent inter-ocean exchange, *Deep Sea Res., Part II*, *50*, 57–86, doi:10.1016/S0967-0645(02)00379-X.

Brunelle, B. (2009), Nitrogen isotope constraints on the biogeochemistry and paleoclimatology of the subarctic North Pacific, PhD thesis, Princeton Univ.

Buchwald, C., and K. Casciotti (2013), Isotopic ratios of nitrite as tracers of the sources and age of oceanic nitrite, *Nat. Geosci.*, *6*, 308–313, doi:10.1038/NGEO1745.

Buchwald, C., A. Santoro, M. McIlvin, and K. Casciotti (2012), Oxygen isotopic composition of nitrate and nitrite produced by nitrifying cocultures and natural marine assemblages, *Limnol. Oceanogr.*, *57*(5), 1361–1375, doi:10.4319/lo.2012.57.5.1361.

Callahan, J. (1972), The structure and circulation of deep water in the Antarctic, *Deep-Sea Res. Oceanogr. Abstr.*, *19*(8), 563–575, doi:10.1016/0011-7471(72)90040-X.

Casciotti, K. (2009), Inverse kinetic isotope fractionation during bacterial nitrite oxidation, *Geochim. Cosmochim. Acta*, *73*, 2061–2076, doi:10.1016/j.gca.2008.12.022.

Casciotti, K., D. Sigman, M. Galanter Hastings, J. Böhlke, and A. Hilkert (2002), Measurement of the oxygen isotopic composition of nitrate in seawater and freshwater using the denitrifier method, *Anal. Chem.*, *74*, 4905–4912, doi:10.1021/ac020113w.

Casciotti, K., D. Sigman, and B. Ward (2003), Linking diversity and stable isotope fractionation in ammonia-oxidizing bacteria, *Geomicrobiol. J.*, *20*, 335–353, doi:10.1080/01490450390241035.

Casciotti, K., J. Böhlke, M. McIlvin, S. Mroczkowski, and J. Hannon (2007), Oxygen isotopes in nitrite: Analysis, calibration, and equilibration, *Anal. Chem.*, *79*, 2427–2436, doi:10.1021/ac061598h.

Checkley, D., and C. Miller (1989), Nitrogen isotope fractionation by oceanic zooplankton, *Deep-Sea Res., Part A*, *36*, 1449–1456, doi:10.1016/0198-0149(89)90050-2.

de Boyer Montégut, C., G. Madec, A. Fischer, A. Lazar, and D. Iudicone (2004), Mixed layer depth over the global ocean: An examination of profile data and a profile-based climatology, *J. Geophys. Res.*, *109*, C12003, doi:10.1029/2004JC002378.

DiFiore, P., D. Sigman, T. Trull, M. Lourey, K. Karsh, G. Cane, and R. Ho (2006), Nitrogen isotope constraints on subantarctic biogeochemistry, *J. Geophys. Res.*, *111*, C08016, doi:10.1029/2005JC003216.

DiFiore, P., D. Sigman, and R. Dunbar (2009), Upper ocean nitrogen fluxes in the Polar Antarctic Zone: Constraints from the nitrogen and oxygen isotopes of nitrate, *Geochem. Geophys. Geosyst.*, *10*, Q11016, doi:10.1029/2009GC002468.

DiFiore, P., D. Sigman, K. Karsh, T. Trull, R. Dunbar, and R. Robinson (2010), Poleward decrease in the isotope effect of nitrate assimilation across the Southern Ocean, *Geophys. Res. Lett.*, *37*, L17601, doi:10.1029/2010GL044090.

Dugdale, R., and J. Goering (1967), Uptake of new and regenerated forms of nitrogen in primary productivity, *Limnol. Oceanogr.*, *12*(2), 196–206, doi:10.4319/lo.1967.12.2.0196.

Eppley, R., and B. Peterson (1979), Particulate organic matter flux and planktonic new production in the deep ocean, *Nature*, *282*, 677–680, doi:10.1038/282677a0.

Eriksen, R. (1997), A practical manual for the determination of salinity, dissolved oxygen, and nutrients in seawater, no. 11 in Research Report, 83 pp., Antarctic CRC, Hobart, Tasmania, Australia.

Fawcett, S., M. Lomas, J. Casey, B. Ward, and D. Sigman (2011), Assimilation of upwelled nitrate by small eukaryotes in the Sargasso Sea, *Nat. Geosci.*, *4*, 717–722, doi:10.1038/NGEO1265.

Fawcett, S., M. Lomas, B. Ward, and D. Sigman (2014), The counterintuitive effect of summer-to-fall mixed layer deepening on eukaryotic new production in the Sargasso Sea, *Global Biogeochem. Cycles*, *28*, 86–102, doi:10.1002/2013GB004579.

Fripiat, F., D. Sigman, S. Fawcett, P. Rafter, M. Weigand, and J.-L. Tison (2014), New insights into sea ice nitrogen biogeochemical dynamics from the nitrogen isotopes, *Global Biogeochem. Cycles*, *28*, 115–130, doi:10.1002/2013GB004729.

Gordon, A., H. Taylor, and D. Georgi (1977), Antarctic oceanographic zonation, in *Polar Oceans*, edited by M. Dunbar, Arctic Institute of North America, Calgary, Alberta, Canada.

Granger, J., and D. Sigman (2009), Removal of nitrite with sulfamic acid for nitrate N and O isotope analysis with the denitrifier method, *Rapid Commun. Mass Spectrom.*, *23*, 3753–3762, doi:10.1002/rcm.4307.

Granger, J., D. Sigman, J. Needoba, and P. Harrison (2004), Coupled nitrogen and oxygen isotope fractionation of nitrate during assimilation by cultures of marine phytoplankton, *Limnol. Oceanogr.*, *49*(5), 1763–1773, doi:10.4319/lo.2004.49.5.1763.

Granger, J., D. Sigman, M. Prokopenko, M. Lehmann, and P. Tortell (2006), A method for nitrite removal in nitrate N and O isotope analyses, *Limnol. Oceanogr. Methods*, *4*, 205–212, doi:10.4319/lom.2006.4.205.

Granger, J., D. Sigman, M. Rohde, M. Maldonado, and P. Tortell (2010), N and O isotope effects during nitrate assimilation by unicellular prokaryotic and eukaryotic plankton cultures, *Geochim. Cosmochim. Acta*, *74*, 1030–1040, doi:10.1016/j.gca.2009.10.044.

Hayes, J. (2002), *Practice and Principles of Isotopic Measurements in Organic Geochemistry (revision 2)*, pp. 1–25, Woods Hole Oceanographic Institution, Woods Hole, Mass.

Holliday, N., and J. Read (1998), Surface oceanic fronts between Africa and Antarctica, *Deep Sea Res., Part I*, *45*, 217–238, doi:10.1016/S0967-0637(97)00081-2.

Joubert, W., S. Thomalla, H. Waldron, M. Lucas, M. Boye, F. Le Moigne, F. Planchon, and S. Speich (2011), Nitrogen uptake by phytoplankton in the Atlantic sector of the Southern Ocean during late austral summer, *Biogeosciences*, *8*, 2947–2959, doi:10.5194/bg-8-2947-2011.

Karsh, K. (2013), Physiological and environmental controls on the nitrogen and oxygen isotope fractionation of nitrate during its assimilation by marine phytoplankton, PhD thesis, Princeton Univ., USA, and CSIRO, Australia.

Karsh, K., T. Trull, M. Lourey, and D. Sigman (2003), Relationship of nitrogen isotope fractionation to phytoplankton size and iron availability during the Southern Ocean Iron RElease Experiment (SOIREE), *Limnol. Oceanogr.*, *48*(3), 1058–1068, doi:10.4319/lo.2003.48.3.1058.

Lehmann, M., S. Bernasconi, A. Barbieri, and J. McKenzie (2002), Preservation of organic matter and alteration of its carbon and nitrogen isotope composition during simulated and in situ early sedimentary diagenesis, *Geochim. Cosmochim. Acta*, *66*(20), 3573–3584, doi:10.1016/S0016-7037(02)00968-7.

Lourey, M., T. Trull, and D. Sigman (2003), Sensitivity of δ^{15}N of nitrate, surface suspended and deep sinking particulate nitrogen to seasonal nitrate depletion in the Southern Ocean, *Global Biogeochem. Cycles*, *17*(3), 1–18, doi:10.1029/2002GB001973.

Lutjeharms, J., and R. van Ballegooyen (1988), The retroflection of the Agulhas Current, *J. Phys. Oceanogr.*, *18*, 1570–1583, doi:10.1175/1520-0485(1988)018<1570:TROTAC>2.0.CO;2.

Mariotti, A., J. Germon, P. Hubert, P. Kaiser, R. Letolle, A. Tardieux, and P. Tardieux (1981), Experimental determination of nitrogen kinetic isotope fractionation: Some principles; illustration for the denitrification and nitrification processes, *Plant Soil*, *62*, 413–430, doi:10.1007/BF02374138.

Möbius, J. (2013), Isotope fractionation during nitrogen remineralization (ammonification): Implications for nitrogen isotope biogeochemistry, *Geochim. Cosmochim. Acta*, *105*, 422–432, doi:10.1016/j.gca.2012.11.048.

Montoya, J., and J. McCarthy (1995), Isotopic fractionation during nitrate uptake by phytoplankton grown in continuous culture, *J. Plankton Res.*, *17*(3), 439–464, doi:10.1093/plankt/17.3.439.

Needoba, J., and P. Harrison (2004), Influence of low light and a light: Dark cycle on NO_3^- uptake, intracellular NO_3^-, and nitrogen isotope fractionation by marine phytoplankton, *J. Phycol.*, *40*, 505–516, doi:10.1111/j.1529-8817.2004.03171.x.

Needoba, J., N. Waser, P. Harrison, and S. Calvert (2003), Nitrogen isotope fractionation in 12 species of marine phytoplankton during growth on nitrate, *Mar. Ecol. Prog. Ser.*, *225*, 81–91, doi:10.3354/meps255081.

Needoba, J., D. Sigman, and P. Harrison (2004), The mechanism of isotope fractionation during algal nitrate assimilation as illuminated by the $^{15}N/^{14}N$ of intracellular nitrate, *J. Phycol.*, *40*, 517–522, doi:10.1111/j.1529-8817.2004.03172.x.

Newell, S., S. Fawcett, and B. Ward (2013), Depth distribution of ammonia oxidation rates and ammonia-oxidizer community composition in the Sargasso Sea, *Limnol. Oceanogr.*, *58*(4), 1491–1500, doi:10.4319/lo.2013.58.4.1491.

Olson, R. (1981), Differential photoinhibition of marine nitrifying bacteria: A possible mechanism for the formation of the primary nitrite maximum, *J. Mar. Res.*, *39*, 227–238.

Orsi, A., and T. Whitworth III (2005), *Hydrographic Atlas of the World Ocean Circulation Experiment (WOCE). Volume 1: Southern Ocean*, International WOCE Project Office, Southampton, U. K., isbn:0-904175-49-9.

Orsi, A., T. Whitworth, and W. Nowlin (1995), On the meridional extent and fronts of the Antarctic Circumpolar Current, *Deep Sea Res., Part I*, *42*(5), 641–673, doi:10.1016/0967-0637(95)00021-W.

Park, Y., L. Gamberoni, and E. Charriaud (1993), Frontal structure, water masses, and circulation in the Crozet Basin, *J. Geophys. Res.*, *98*(C7), 12,361–12,385, doi:10.1029/93JC00938.

Priscu, J., M. Downes, L. Priscu, A. Palmisano, and C. Sullivan (1990), Dynamics of ammonium oxidizer activity and nitrous oxide (N_2O) within and beneath Antarctic sea ice, *Mar. Ecol. Prog. Ser.*, *62*, 37–46, doi:10.3354/meps062037.

Rafter, P., P. DiFiore, and D. Sigman (2013), Coupled nitrate nitrogen and oxygen isotopes and organic matter remineralization in the Southern and Pacific Oceans, *J. Geophys. Res. Oceans*, *118*, 4781–4794, doi:10.1002/jgrc.20316.

Riaux-Gobin, C., P. Tréguer, G. Dieckmann, E. Maria, G. Vétion, and M. Poulin (2005), Land-fast ice off Adélie Land (Antarctica): Short-term variations in nutrients and chlorophyll just before ice breakup, *J. Mar. Syst.*, *55*, 235–248, doi:10.1016/j.jmarsys.2004.08.003.

Sarmiento, J., and J. Toggweiler (1984), A new model for the role of the oceans in determining atmospheric pCO_2, *Nature*, *308*, 621–624, doi:10.1038/308621a0.

Sarmiento, J., et al. (2004), Response of ocean ecosystems to climate warming, *Global Biogeochem. Cycles*, *18*, GB3003, 1–23, doi:10.1029/2003GB002134.

Schmid, C., O. Boebel, J. Lutjeharms, S. Garzoli, P. Richardson, and C. Barron (2003), Early evolution of an Agulhas Ring, *Deep Sea Res., Part II*, *50*, 141–166, doi:10.1016/S0967-0645(02)00382-X.

Sigman, D., M. Altabet, D. McCorkle, R. François, and G. Fischer (1999), The δ^{15}N of nitrate in the Southern Ocean: Consumption of nitrate in surface waters, *Global Biogeochem. Cycles*, *13*(4), 1149–1166, doi:10.1029/1999GB900038.

Sigman, D., M. Altabet, D. McCorkle, R. François, and G. Fischer (2000), The δ^{15}N of nitrate in the Southern Ocean: Nitrogen cycling and circulation in the ocean interior, *J. Geophys. Res.*, *105*(C8), 19,599–19,614, doi:10.1029/2000JC000265.

Sigman, D., K. Casciotti, M. Andreani, C. Barford, M. Galanter, and J. Böhlke (2001), A bacterial method for the nitrogen isotopic analysis of nitrate in seawater and freshwater, *Anal. Chem.*, *73*, 4145–4153, doi:10.1021/ac010088e.

Sigman, D., K. Karsh, and K. Casciotti (2009a), Ocean process tracers: Nitrogen isotopes in the ocean, *Encyclopedia of Ocean Sciences*, pp. 4138–4152, 2nd ed., Elsevier, Amsterdam.

Sigman, D., P. DiFiore, M. Hain, C. Deutsch, and D. Karl (2009b), Sinking organic matter spreads the nitrogen isotope signal of pelagic denitrification in the North Pacific, *Geophys. Res. Lett.*, *36*, L08605, doi:10.1029/2008GL035784.

Sigman, D., P. DiFiore, M. Hain, C. Deutsch, Y. Wang, D. Karl, A. Knapp, M. Lehmann, and S. Pantoja (2009c), The dual isotopes of deep nitrate as a constraint on the cycle and budget of oceanic fixed nitrogen, *Deep Sea Res., Part I*, *56*, 1419–1439, doi:10.1016/j.dsr.2009.04.007.

Smart, S. (2014), Wintertime nitrate isotope dynamics in the Atlantic sector of the Southern Ocean, Master's thesis, Univ. of Cape Town, South Africa.

Smith, J., F. Chavez, and C. Francis (2014), Ammonium uptake by phytoplankton regulates nitrification in the sunlit ocean, *PLoS One*, *9*(9), e108,173, doi:10.1371/journal.pone.0108173.

Strickland, J., and T. Parsons (1972), *A Practical Handbook of Seawater Analysis*, vol. 167, 2nd ed., pp. 1–310, Bulletin of the Fisheries Research Board of Canada, Ottawa, Canada.

Swart, S., S. Thomalla, P. Monteiro, and I. Ansorge (2012), Mesoscale features and phytoplankton biomass at the GoodHope line in the Southern Ocean during austral summer, *Afr. J. Mar. Sci.*, *34*(4), 511–524, doi:10.2989/1814232X.2012.749811.

Thomalla, S., N. Fauchereau, S. Swart, and P. Monteiro (2011), Regional scale characteristics of the seasonal cycle of chlorophyll in the Southern Ocean, *Biogeosciences*, *8*, 2849–2866, doi:10.5194/bg-8-2849-2011.

Trull, T., D. Davies, and K. Casciotti (2008), Insights into nutrient assimilation and export in naturally iron-fertilized waters of the Southern Ocean from nitrogen, carbon, and oxygen isotopes, *Deep Sea Res., Part II*, *55*, 820–840, doi:10.1016/j.dsr2.2007.12.035.

Wada, E., and A. Hattori (1978), Nitrogen isotope effects in the assimilation of inorganic nitrogenous compounds by marine diatoms, *Geomicrobiol. J.*, *1*(1), 85–101, doi:10.1080/01490457809377725.

Ward, B. (2005), Temporal variability in nitrification rates and related biogeochemical factors in Monterey Bay, California, USA, *Mar. Ecol. Prog. Ser.*, *292*, 97–109, doi:10.3354/meps292097.

Waser, N., P. Harrison, B. Nielsen, S. Calvert, and D. Turpin (1998), Nitrogen isotope fractionation during the uptake and assimilation of nitrate, nitrite, ammonium, and urea by a marine diatom, *Limnol. Oceanogr.*, *43*(2), 215–224, doi:10.4319/lo.1998.43.2.0215.

Whitworth, T. (1980), Zonation and geostrophic flow of the Antarctic Circumpolar Current at Drake Passage, *Deep-Sea Res., Part A*, *27*(7), 497–507, doi:10.1016/0198-0149(80)90036-9.

Whitworth, T., and W. Nowlin (1987), Water masses and currents of the Southern Ocean at the Greenwich meridian, *J. Geophys. Res.*, *92*(C6), 6462–6476, doi:10.1029/JC092iC06p06462.

Wu, J., S. Calvert, and C. Wong (1997), Nitrogen isotope variations in the subarctic northeast Pacific: Relationships to nitrate utilization and trophic structure, *Deep Sea Res., Part I*, *44*(2), 287–314, doi:10.1016/S0967-0637(96)00099-4.

Yool, A., A. Martin, C. Fernández, and D. Clark (2007), The significance of nitrification for oceanic new production, *Nature*, *447*, 999–1002, doi:10.1038/nature05885.

Yoshikawa, C., Y. Yamanaka, and T. Nakatsuka (2006), Nitrate-nitrogen isotopic patterns in surface waters of the western and central equatorial Pacific, *J. Oceanogr.*, *62*, 511–525, doi:10.1007/s10872-006-0072-4.